Web crippling behaviour of cold-formed steel channel sections having elongated edge-stiffened web holes under interior-two-flange loading condition

Wei Wang [a], Krishanu Roy [a]*, Zhiyuan Fang[a]*, Beulah Gnana Ananthi[b], James B.P. Lim[a]*

[a] School of Engineering, The University of Waikato, New Zealand

[b] Division of Structural Engineering, Anna University, India

*Corresponding author: Krishanu Roy, Zhiyuan Fang, James B.P. Lim

Abstract: In the past decade, cold-formed steel (CFS) channel sections having circular edge-stiffened web holes have been developed in New Zealand. Such edge-stiffened holes increase the strength of the CFS channel sections, compared to an equivalent section having unstiffened holes, while still allowing full service integration. In the case of web crippling, previous research has found that use of edge-stiffened holes almost results in the same strength of an equivalent channel-section having a plain web. Such circular edge-stiffened web holes can now be extended to elongated edge-stiffened web holes. However, for such elongated holes, no experimental tests have been reported in the literature. In this paper, a numerical investigation was carried out, and non-linear finite element (FE) analyses were used to investigate the web crippling behaviour of CFS channel sections having edge-stiffened web holes under the interior-two-flange (ITF) loading condition. The cases of both flange fastened and flange unfastened were considered. The FE models were validated against test results of sections having circular edge-stiffened web holes; good agreement in terms of the load-displacement curves and deformed shapes was shown. Using the validated FE models, a parametric study was carried out on CFS channel sections having elongated un-stiffened and edge-stiffened web holes, comprising 1,227 finite element analyses (FEA) results. Compared to sections having a plain web, for the case of an elongated opening, without any edge-stiffener, having an aspect ratio of two and three, the average reduction in web crippling strength was 39% and 49%, respectively. However, for an edge-stiffened hole, the reduction in the web crippling strength was reduced to only 2% and 16%, respectively.

Finally, the design equations in the form of the web crippling reduction factor (R_p) and the equations based on the direct strength method (DSM) for CFS sections with elongated web holes were proposed.

Keywords: Cold-formed steel; Web crippling; Edge-stiffened web holes; Elongated web holes; Interior-two-flange; Finite element analysis; Direct strength method

1 Introduction

Cold-formed steel (CFS) channel-sections often require holes in the webs in order to allow services to be integrated within the floors. Such holes, however, result in the channel sections becoming susceptible to web crippling (see Fig. 1) in the vicinity of a concentrated load [1-3].

Over the last decade, a new generation of CFS channel sections having circular edge-stiffened web holes has been developed in New Zealand [3] (see Fig. 2). Experimental tests on such sections have been reported in the literature considering, in addition to web crippling [1, 2], compression [5, 6], bending [7, 8] and shear [9, 10]; design recommendations for each of these have been proposed.

However, in some cases, it is necessary for elongated web holes to be used, in order for larger services to be accommodated (see Fig. 3). As with the circular web holes, these elongated web holes can be edge-stiffened. Fig. 4 shows the parameters adopted in this paper to describe an elongated web hole. No previous research, however, has been reported on their web crippling behaviour. This paper addresses this issue, specifically for the interior-two-flange (ITF) loading condition (see Fig. 5).

In terms the literature of web crippling of CFS channel sections having circular edge-stiffened web holes, experimental and numerical studies have been reported by Uzzaman et al. [1] and Chen et al. [2] on the web crippling behaviour of CFS channel sections having circular un-stiffened and edge-stiffened web holes under the ITF loading condition. Chen et al. [2] considered the case of flanges fastened to bearing plates, and the

54 results indicated that the web crippling capacity increased by 33% under the ITF loading
55 condition compared to flanges unfastened. However, neither Uzzaman et al. [1] nor Chen et
56 al. [2] considered elongated web holes.

57 In terms of the design standards, i.e., AISI S100 (2016) [11], AS/NZS 4600 (2018) [12]
58 and EC3 (2006) [13], no guidance is provided for CFS channel sections having unstiffened
59 and edge-stiffened web holes under web crippling.

60 In terms of the literature, the strength reduction factor (R_P) was normally used to quantify
61 the influence of web holes, and R_P is equal to the web crippling strengths of sections having
62 web holes divided by that of plain sections. For circular web holes, some researchers [1,
63 14-20] proposed web crippling design recommendations in the form of R_P equations based on
64 extensive experimental and numerical studies. However, these design recommendations [1,
65 14-20] are not applicable to elongated holes

66 This paper presents a numerical study using non-linear elastic-plastic finite element
67 analysis (FEA) to investigate the effect of elongated edge-stiffened web holes on the web
68 crippling strength of CFS channels sections under ITF loading condition; the study also
69 includes elongated un-stiffened web holes. The finite element (FE) models were validated
70 against the experimental results reported by Chen et al. [2] on circular edge-stiffened web
71 holes. Using the validated FE models, the results of 1,227 FEA, 1,051 of which were for
72 parameter studies and 176 for elastic critical buckling analyses, are presented on elongated
73 web holes; the cases of both flanges fastened and unfastened to bearing plates are considered.
74 From the results of the parametric study, design equations for the web crippling strength

reduction factor were proposed. In addition, for the case of CFS channel sections with unfastened flanges, a direct strength method (DSM) equation was also proposed to determine ITF web crippling strength considering the effects of elongated un-stiffened and edge-stiffened web holes.

Finally, the reliability of all the proposed design methods was demonstrated by means of statistical analyses, showing their suitability for incorporation into future revisions of international design codes for cold-formed steel structures.

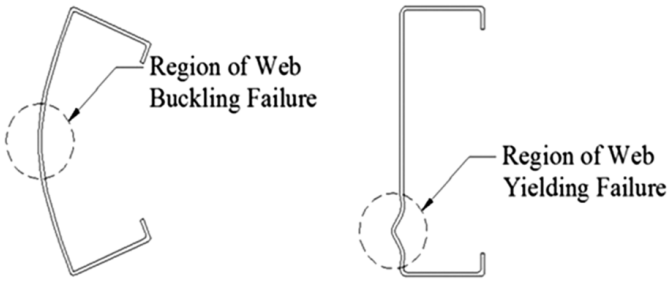

(a) Web buckling (b) Web yielding

Fig. 1 Web crippling [3]

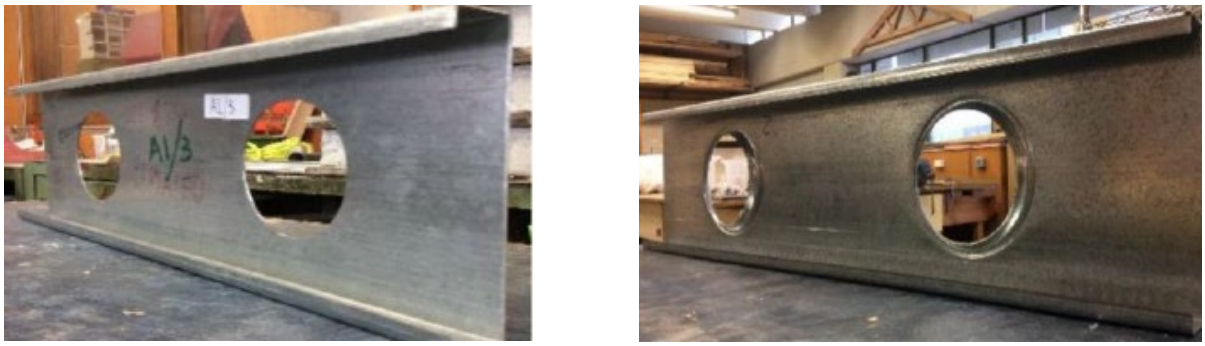

(a) Un-stiffened holes (b) Edge-stiffened web holes

Fig. 2 CFS channel sections with circular web holes [1]

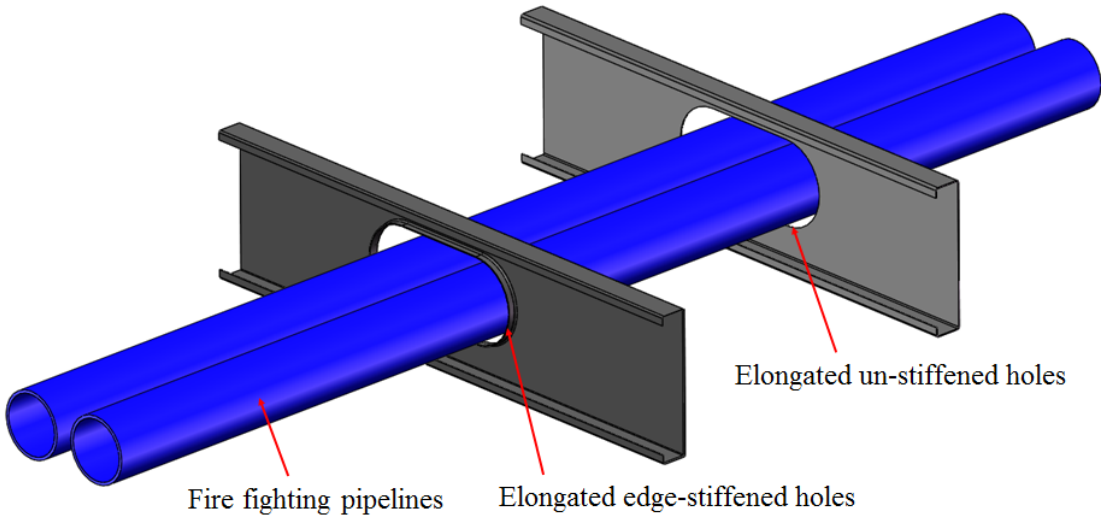

Fig. 3 Elongated web holes for building services

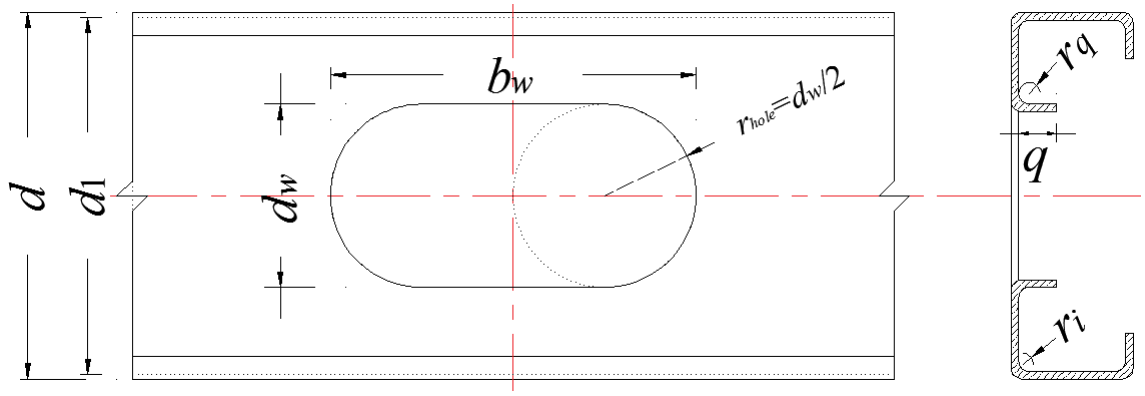

Fig. 4 Elongated edge-stiffened web holes details

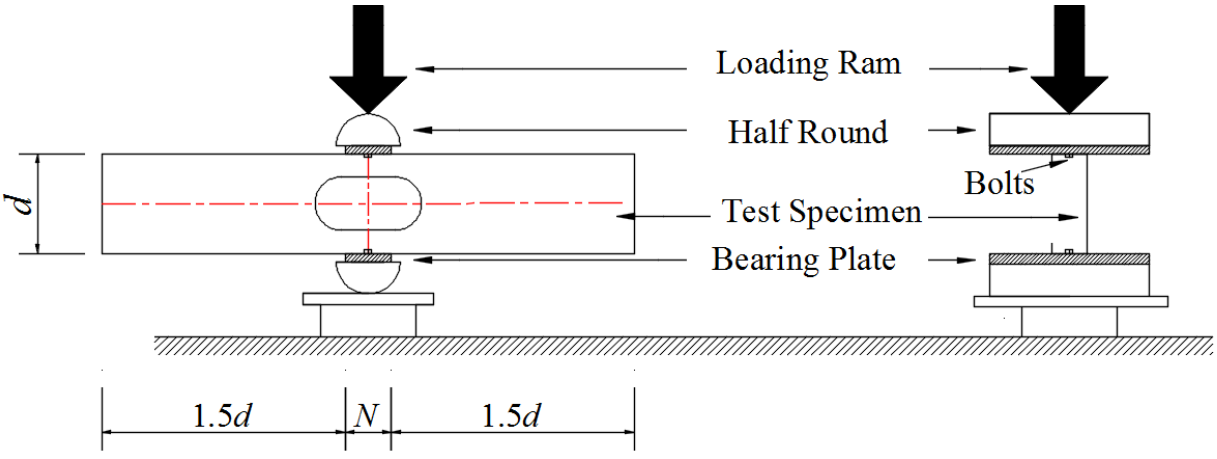

Fig. 5 ITF loading condition with fastened flanges

2 Summary of research by Chen et al. [2]

2.1 General

As mentioned in the Introduction, no experimental study was found in the literature on the web crippling behaviour of CFS channel sections having elongated un-stiffened and edge-stiffened web holes. Therefore, the results of web crippling tests (Table 1 and Fig. 6) on CFS channel sections having circular web holes under ITF loading condition reported by Chen et al. [2] were used to validate the FE models developed in this paper. Further test details can be found in Chen et al. [2]. The modelling techniques described by Chen et al. [2] were used. For completeness, these are described in the following subsections.

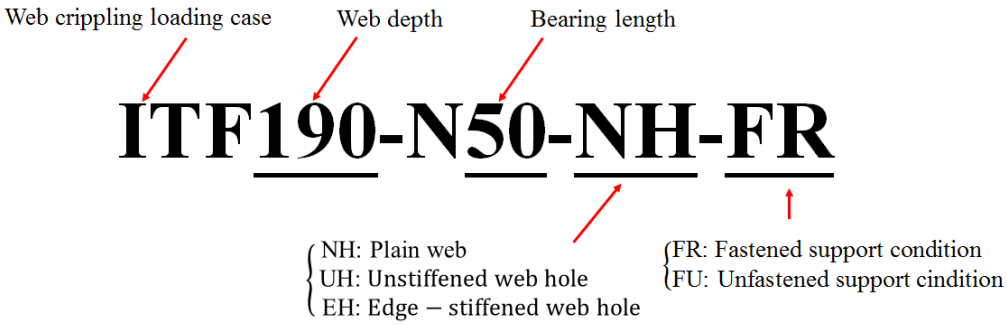

Fig. 6 Specimen labelling for tests reported by Chen et al. [2]

Table 1 Specimen dimensions and experimental ultimate loads [2]

Specimens	Web d (mm)	Flange b_f (mm)	Lip b_t (mm)	Length L (mm)	Bearing length N (mm)	Stiffener length q (mm)	Exp. load P_{EXP} (kN)	FEA. load P_{FEA} (kN)	P_{EXP}/P_{FEA}
(a) Fastened support									
ITF190-N50-NH-FR	190.5	44.9	15.00	620.50	50	-	11.30	10.78	1.05
ITF190-N75-NH-FR	189.5	45.3	14.80	645.50	75	-	11.82	11.82	1.00
ITF190-N100-NH-FR	190.3	45.5	15.30	670.00	100	-	12.20	11.69	1.04
ITF190-N50-UH-FR	189.7	45.3	15.00	620.00	50	-	8.62	8.89	0.97
ITF190-N75-UH-FR	190.5	44.8	14.80	645.50	75	-	8.75	9.00	0.97
ITF190-N100-UH-FR	190.0	45.0	15.30	670.30	100	-	8.92	9.32	0.96
ITF190-N50-EH-FR	190.0	45.0	15.00	620.20	50	13	10.71	10.79	0.99
ITF190-N75-EH-FR	190.5	44.6	15.30	645.30	75	13	11.23	11.68	0.96

ITF190-N100-EH-FR	189.5	45.5	14.90	669.50	100	13	11.55	11.81	0.98
(b) Unfastened support									
ITF190-N50-UH-FU	190.5	45.2	14.80	620.50	50	-	8.27	8.16	1.01
ITF190-N75-UH-FU	190.3	45.0	15.00	645.00	75	-	8.78	8.28	1.06
ITF190-N100-UH-FU	190.5	44.8	15.10	670.50	100	-	9.21	9.12	1.01
ITF190-N50-UH-FU	190.0	45.0	14.90	621.00	50	-	6.45	6.39	1.01
ITF190-N75-UH-FU	190.2	45.1	15.50	645.50	75	-	6.64	6.66	1.00
ITF190-N100-UH-FU	190.5	45.5	15.50	670.00	100	-	6.89	6.96	0.99
ITF190-N50-EH-FU	190.5	45.5	15.00	620.50	50	13	7.88	8.12	0.97
ITF190-N75-EH-FU	190.1	45.0	14.80	645.00	75	13	8.29	8.53	0.97
ITF190-N100-EH-FU	190.5	45.3	15.30	670.20	100	13	8.61	8.68	0.99
Mean									1.00
COV									0.03

2.2 Material properties

Material properties were obtained from the tensile coupon tests reported by Chen et al. [2]. As per the ABAQUS manual [21], the engineering material curve was converted into a true material curve by the following equations below:

$$\sigma_{true} = \sigma(1+\varepsilon) \quad (1)$$

$$\varepsilon_{true(pl)} = \ln(1+\varepsilon) - \frac{\sigma_{true}}{E} \quad (2)$$

Where σ_{true} and $\varepsilon_{true(pl)}$ are the true stress and plastic strain, respectively, while σ and ε are the engineering stress and strain, and E represents the elastic modulus.

2.3 Element type and mesh sensitivity

S4R shell elements with six degrees of freedom per node were used to model the CFS channel sections, while R3D4 rigid elements were chosen to model the bearing plates. Based on mesh sensitivity analysis results, a mesh size of 10 mm × 10 mm was used to simulate the bearing plates, while a mesh size of 5 mm × 5 mm was found to be appropriate for the channel sections. Mesh refinement was used around the elongated web holes and the channel

106 section corners between the web and flanges. The FE meshing details were presented in Fig.

107 7.

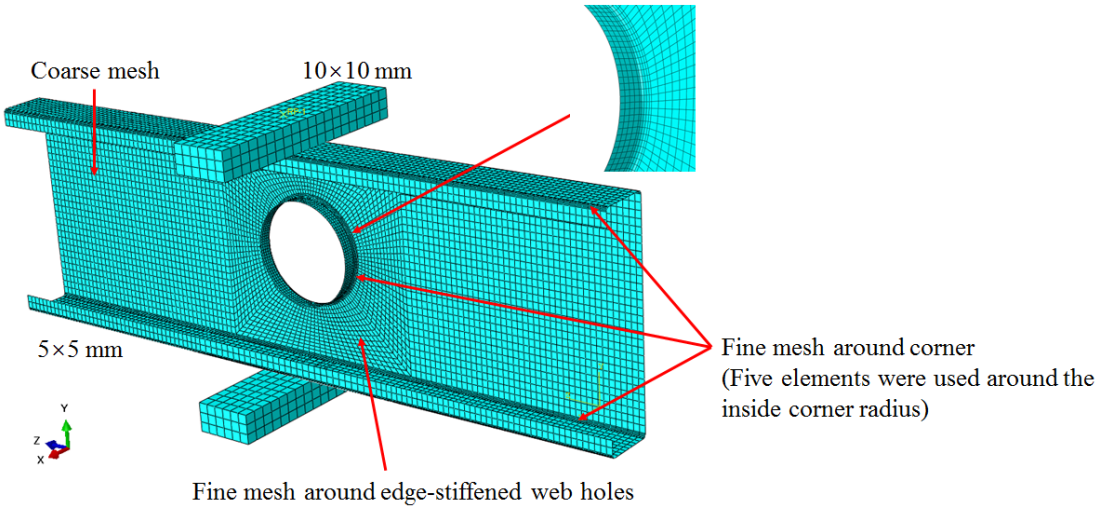

Fig. 7 Mesh sizes of different regions

108 *2.4 Interactions and boundary conditions*

109 The interface between the CFS channel sections and the bearing plates was modelled by

110 employing "Surface-to-Surface" contact, available in ABAQUS [20]. The bearing plate with

111 the higher stiffness was chosen as the master surface, and the flanges of the channel were

112 selected as the slave surface. The discretization method employed the "node-to-surface"

113 approach to avoid the penetration of two contact surfaces. Apart from the degrees of freedom

114 associated with the direction of loading, all other degrees of freedom were constrained at the

115 top bearing plate. Displacement control was used to apply the axial load through a reference

116 point at the top bearing plate (see Fig. 8). For the case of the fastened flanges, a "Cartesian"

117 connector in ABAQUS [20] was employed to model the bolt connections. The Cartesian

118 connector is a special type of connector element that is defined by three nodes and is suitable

for various types of rigid linkages. The connector allows the user to prescribe translational and rotational degrees of freedom and axial stiffness between the connected nodes.

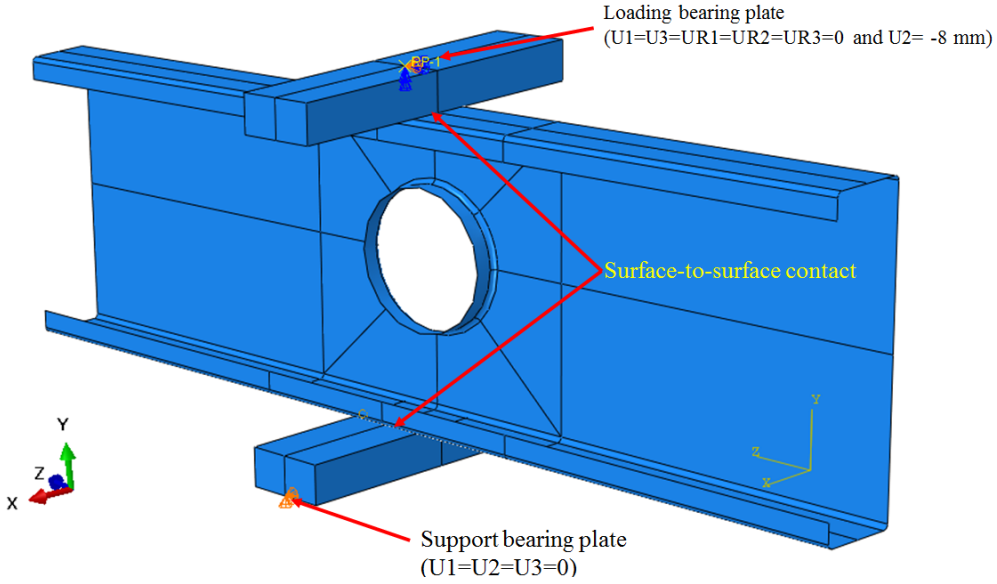

Fig. 8 Boundary conditions and interactions used in variation model

2.5 Validation of the FE models

A comparison of the experimental results (P_{EXP}) of Chen et al. [2] with the FEA results (P_{FEA}) reported in this paper was summarized in Table 1. The specimens [2] were labelled as shown in Fig. 6. As can be seen from Table 1, the mean value of the ratio P_{EXP}/P_{FEA} is 1.00 with the corresponding coefficient of variation (COV) of 0.03. Figs. 9 and 10 show the comparison of load-displacement curves and deformed shapes obtained from the FEA and experimental results [2]. From Figs. 9 and 10, it can be seen that the deformed shapes and the load-displacement curves of FEA and tests could match each other well. Overall, the FE model developed in this paper showed good correlation against the experimental results.

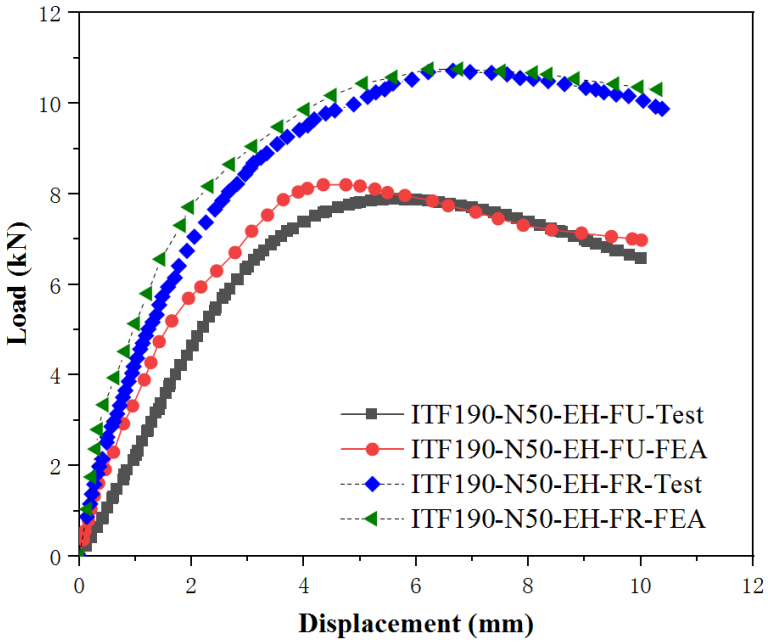

Fig. 9 Comparison of load-displacement curve for the specimens ITF190-N50-EH

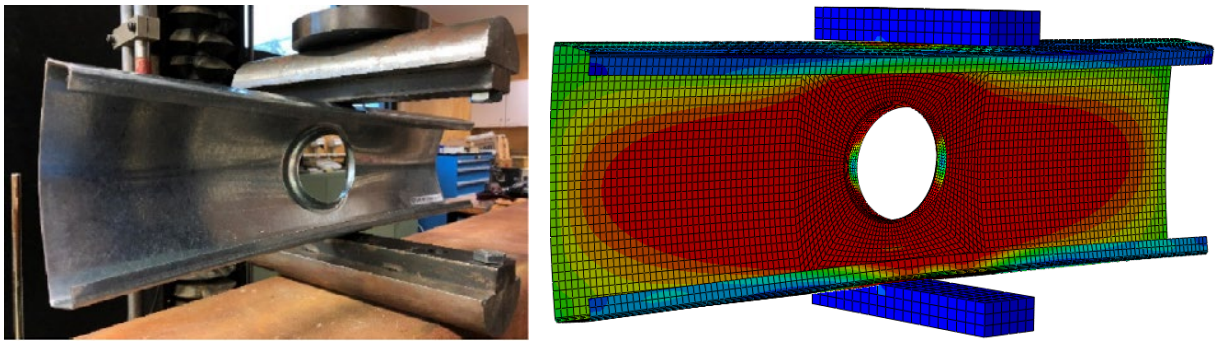

(a) ITF190-N50-EH-FU-Test [2] (b) ITF190-N50-EH-FU-FEA

Fig. 10 Comparison of deformed shape for the specimen ITF190-N50-EH-FU

3 Parametric study

Using the same finite element modelling techniques described in Seciton 2, a parametric study was conducted on CFS channel sections having elongated un-stiffened and edge-stiffened web holes (see Figs. 3 and 11) under the ITF loading condition. Two channel sections reported in the literatures [2, 7], were used in the parametric study to investigate the effects of the ratio of width of holes to depth of flat portion of web (d_w/d_1), length to width of

holes (b_w/d_w), edge-stiffener length to depth of flat portion of web (q/d_1), the bearing length to thickness of sections (N/t), and inside fillet radius between web and edge-stiffener to depth of flat portion of web (r_q/d_1) on the web crippling strength reduction factor (R_P). For comparison, the cases of unfastened flange and fastened flange were considered in the parametric study.

The values of different parameters investigated in the parametric study are summarized in Table 2, and those specimen dimensions were summarized in Table 3. In Table 4, the web crippling strength of CFS channel sections having plain webs, un-stiffened and edge-stiffened web holes obtained from FEA were summarized. The specimen labelling of the parametric study is shown in Fig. 12.

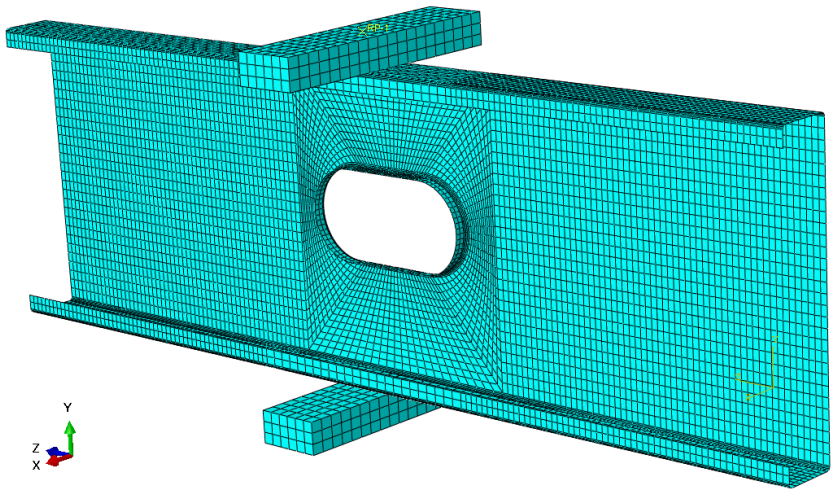

Fig. 11 CFS channel sections having elongated edge-stiffened holes for a parametric study

Table 2 Different parameters used in a parametric study

Sections (mm)	Flange condition	Elongated web holes		Bearing length	Ratio of edge-stiffener length to depth of flat portion of web	Inside fillet radius between web and edge-stiffener
		Ratio of width of holes to depth of flat portion of web	Ratio of length to width of holes			
		d_w/d_1	b_w/d_w	N (mm)	Q (q/d_1)	r_q (mm)
190×45×15-t1.5 [3] 240×45×15-t1.5 [8]	Fastened flange, Unfastened flange	0,0.3,0.5,0.7	2, 2.5, 3	50,75,100	0.02,0.06,0.10	2, 3, 4, 6

147 **Table 3** Details of CFS channel sections investigated in a parametric study

Sections	Web d (mm)	Flange b_f (mm)	Lip b_t (mm)	Length L (mm)	Bearing length N (mm)	Thickness t (mm)
190×45×15-t1.5	190.00	45.00	15.00	620.00	50.00	1.50
190×45×15-t1.5	190.00	45.00	15.00	645.00	75.00	1.50
190×45×15-t1.5	190.00	45.00	15.00	670.00	100.00	1.50
240×45×15-t1.5	240.00	45.00	15.00	770.00	50.00	1.50
240×45×15-t1.5	240.00	45.00	15.00	795.00	75.00	1.50
240×45×15-t1.5	240.00	45.00	15.00	820.00	100.00	1.50

148

149 **Table 4 (a)** Web crippling strength predicted from FEA for CFS channel sections 190×45×15-*t*1.5 with unfastened flanges

Bearing length	Elongated web holes		Web crippling strength per web predicted from FEA, P_{FEA}(kN)											
					With edge-stiffened hole									
					Q0.02		Q0.06				Q0.10			
N (mm)	d_w/d_1	b_w/d_w	Plain web	With un-stiffened hole	r_q=2 (mm)	r_q=3 (mm)	r_q=2 (mm)	r_q=3 (mm)	r_q=4 (mm)	r_q=6 (mm)	r_q=2 (mm)	r_q=3 (mm)	r_q=4 (mm)	r_q=6 (mm)
50.00	0.30	2.00	8.16	7.24	7.58	6.44	7.01	7.03	7.03	7.08	7.20	7.22	7.24	7.30
50.00	0.30	2.50	8.16	6.89	6.15	6.13	6.72	6.74	6.74	6.79	6.99	7.01	7.04	7.12
50.00	0.30	3.00	8.16	6.52	5.83	5.82	6.41	6.43	6.43	6.49	6.73	6.75	6.79	6.88
75.00	0.30	2.00	8.28	6.96	7.62	7.60	8.20	8.21	8.21	8.26	8.45	8.46	8.48	8.52
75.00	0.30	2.50	8.28	6.61	6.78	6.76	7.35	7.36	7.36	7.41	7.65	7.67	7.69	7.76
75.00	0.30	3.00	8.28	6.27	6.45	6.41	7.02	7.03	7.02	7.07	7.35	7.37	7.39	7.46
100.00	0.30	2.00	9.12	7.66	7.69	7.68	8.26	8.27	8.27	8.32	8.50	8.51	8.53	8.59
100.00	0.30	2.50	9.12	7.31	7.36	7.35	7.94	7.95	7.95	7.99	8.24	8.25	8.27	8.34
100.00	0.30	3.00	9.12	6.94	7.05	7.03	7.61	7.62	7.61	7.66	7.94	7.96	7.98	8.05
50.00	0.50	2.00	8.16	5.51	5.32	5.47	6.85	6.89	6.90	7.01	7.26	7.30	7.35	7.50
50.00	0.50	2.50	8.16	4.95	4.95	4.92	6.31	6.34	6.34	6.45	6.70	6.74	6.79	6.94
50.00	0.50	3.00	8.16	4.43	4.44	4.42	5.81	5.84	5.85	5.97	6.18	6.22	6.27	6.40
75.00	0.50	2.00	8.28	5.41	5.67	5.65	6.84	6.87	6.87	6.96	7.23	7.25	7.29	7.39
75.00	0.50	2.50	8.28	4.88	5.13	5.11	6.29	6.32	6.32	6.42	6.67	6.70	6.74	6.86
75.00	0.50	3.00	8.28	4.38	4.62	4.60	5.79	5.82	5.83	5.93	6.15	6.18	6.22	6.33
100.00	0.50	2.00	9.12	6.04	6.22	6.19	7.39	7.42	7.42	7.50	7.77	7.79	7.83	7.93
100.00	0.50	2.50	9.12	5.46	5.66	5.64	6.84	6.87	6.87	6.96	7.22	7.25	7.29	7.39
100.00	0.50	3.00	9.12	4.93	5.16	5.13	6.35	6.37	6.38	6.47	6.71	6.73	6.77	6.89
50.00	0.70	2.00	8.16	3.80	3.95	3.97	6.35	6.41	6.44	6.63	6.66	6.72	6.80	6.99
50.00	0.70	2.50	8.16	3.18	3.53	3.55	5.79	5.84	5.89	6.06	5.99	6.04	6.11	6.30
50.00	0.70	3.00	8.16	2.63	3.00	2.99	5.16	5.18	5.25	5.46	5.34	5.45	5.52	5.67
75.00	0.70	2.00	8.28	3.83	4.12	4.09	6.27	6.32	6.36	6.53	6.61	6.65	6.74	6.92
75.00	0.70	2.50	8.28	3.24	3.63	3.61	5.73	5.79	5.81	5.98	5.98	6.03	6.09	6.26
75.00	0.70	3.00	8.28	2.70	3.17	3.21	5.31	5.37	5.43	5.60	5.55	5.60	5.67	5.82
100.00	0.70	2.00	9.12	4.36	4.62	4.59	6.81	6.86	6.89	7.05	7.14	7.20	7.27	7.45
100.00	0.70	2.50	9.12	3.71	4.01	4.03	6.24	6.30	6.34	6.47	6.51	6.57	6.64	6.81
100.00	0.70	3.00	9.12	3.13	3.59	3.61	5.70	5.75	5.78	5.90	5.93	5.98	6.05	6.18

Table 4 (b) Web crippling strengths predicted from FEA for CFS channel sections 190×45×15-*t*1.5 with fastened flanges

Bearing length	Elongated web holes		Web crippling strength per web predicted from FEA, P_{FEA}(kN)									
				With edge-stiffened hole								
				Q0.02		Q0.06				Q0.10			
N (mm)	d_w/d_1	b_w/d_w	Plain web	r_q=2 (mm)	r_q=3 (mm)	r_q=2 (mm)	r_q=3 (mm)	r_q=4 (mm)	r_q=6 (mm)	r_q=2 (mm)	r_q=3 (mm)	r_q=4 (mm)	r_q=6 (mm)
50.00	0.30	2.00	10.78	9.84	9.83	10.36	10.38	10.39	10.40	10.41	10.43	10.44	10.42
50.00	0.30	2.50	10.78	9.38	9.36	10.23	10.26	10.25	10.32	10.42	10.43	10.41	10.46
50.00	0.30	3.00	10.78	8.88	8.80	9.83	9.88	9.88	9.97	10.22	10.30	10.36	10.45
75.00	0.30	2.00	11.82	9.64	9.61	10.10	10.12	10.13	10.15	10.19	10.21	10.22	10.23
75.00	0.30	2.50	11.82	8.78	8.76	9.41	9.43	9.42	9.49	9.66	9.68	9.71	9.77
75.00	0.30	3.00	11.82	8.70	8.68	9.37	9.38	9.37	9.44	9.72	9.74	9.76	9.84
100.00	0.30	2.00	11.69	9.88	9.86	10.46	10.47	10.46	10.50	10.66	10.66	10.68	10.72
100.00	0.30	2.50	11.69	9.55	9.53	10.19	10.19	10.18	10.23	10.46	10.48	10.50	10.56
100.00	0.30	3.00	11.69	9.22	9.21	9.89	9.91	9.90	9.96	10.23	10.25	10.28	10.35
50.00	0.50	2.00	10.78	7.77	7.82	9.74	9.79	9.77	10.02	10.39	10.43	10.50	10.63
50.00	0.50	2.50	10.78	7.78	7.86	8.90	8.99	8.98	9.23	9.53	9.60	9.69	9.94
50.00	0.50	3.00	10.78	7.67	7.03	8.35	8.38	8.38	8.53	8.71	8.76	8.82	9.04
75.00	0.50	2.00	11.82	7.42	7.48	8.94	8.98	8.98	9.11	9.31	9.36	9.41	9.55
75.00	0.50	2.50	11.82	7.35	7.39	8.51	8.55	8.56	8.70	8.90	8.95	9.01	9.17
75.00	0.50	3.00	11.82	7.01	7.12	8.11	8.14	8.15	8.28	8.44	8.48	8.53	8.70
100.00	0.50	2.00	11.69	8.19	8.22	9.70	9.74	9.74	9.87	10.08	10.13	10.19	10.33
100.00	0.50	2.50	11.69	5.47	5.45	6.57	6.65	6.66	6.83	7.12	7.16	7.20	7.27
100.00	0.50	3.00	11.69	7.74	7.76	8.87	8.90	8.90	9.03	9.23	9.27	9.32	9.45
50.00	0.70	2.00	10.78	6.82	6.88	8.56	8.60	8.76	8.92	8.77	8.84	8.94	9.13
50.00	0.70	2.50	10.78	5.58	5.59	7.82	7.85	7.88	8.01	7.96	7.97	7.98	8.18
50.00	0.70	3.00	10.78	4.81	4.83	7.08	7.11	6.95	6.99	7.31	7.49	7.50	7.54
75.00	0.70	2.00	11.82	6.57	6.61	8.43	8.45	8.41	8.57	8.81	8.85	8.90	9.02
75.00	0.70	2.50	11.82	5.74	5.72	7.72	7.76	7.75	7.90	8.01	8.05	8.06	8.15
75.00	0.70	3.00	11.82	4.51	4.22	6.91	6.96	6.94	6.97	7.17	7.23	7.24	7.31
100.00	0.70	2.00	11.69	7.11	7.30	9.29	9.33	9.30	9.44	9.64	9.68	9.72	9.86
100.00	0.70	2.50	11.69	6.25	6.49	8.56	8.59	8.55	8.64	8.83	8.82	8.89	8.94
100.00	0.70	3.00	11.69	5.39	5.22	7.67	7.62	7.71	7.67	7.88	7.91	7.96	8.01

Table 4 (c) Web crippling strength predicted from FEA for CFS channel sections 240×45×15-t1.5 with unfastened flanges

Bearing length N (mm)	Elongated web holes		Web crippling strength per web predicted from FEA, P_{FEA}(kN)											
			Plain web	With un-stiffened hole	With edge-stiffened hole									
					Q0.02		Q0.06				Q0.10			
	d_w/d_1	b_w/d_w			r_q=2 (mm)	r_q=3 (mm)	r_q=2 (mm)	r_q=3 (mm)	r_q=4 (mm)	r_q=6 (mm)	r_q=2 (mm)	r_q=3 (mm)	r_q=4 (mm)	r_q=6 (mm)
50.00	0.30	2.00	7.50	6.45	8.05	8.04	8.24	8.24	8.25	8.24	8.30	8.30	8.31	8.31
50.00	0.30	2.50	7.50	6.12	7.86	7.84	8.15	8.15	8.15	8.14	8.26	8.26	8.27	8.27
50.00	0.30	3.00	7.50	5.80	7.62	7.60	8.02	8.02	7.99	8.02	8.20	8.19	8.20	8.20
75.00	0.30	2.00	9.45	7.35	7.77	7.74	8.44	8.44	8.43	8.46	8.74	8.75	8.76	8.81
75.00	0.30	2.50	9.45	6.92	7.35	7.32	8.03	8.03	8.02	8.05	8.37	8.38	8.40	8.46
75.00	0.30	3.00	9.45	6.52	6.95	6.93	7.64	7.64	7.62	7.66	7.99	8.01	8.03	8.09
100.00	0.30	2.00	9.52	7.44	7.83	7.81	8.50	8.51	8.50	8.52	8.80	8.81	8.83	8.88
100.00	0.30	2.50	9.52	7.02	7.42	7.40	8.09	8.10	8.08	8.12	8.43	8.44	8.45	8.51
100.00	0.30	3.00	9.52	6.62	7.03	7.00	7.70	7.71	7.70	7.74	8.05	8.06	8.08	8.14
50.00	0.50	2.00	7.50	4.83	6.25	6.23	7.49	7.51	7.49	7.51	7.82	7.85	7.87	7.92
50.00	0.50	2.50	7.50	4.32	5.65	5.65	6.92	6.93	6.91	6.94	7.29	7.30	7.32	7.38
50.00	0.50	3.00	7.50	3.84	5.33	5.29	6.41	6.41	6.41	6.43	6.71	6.72	6.77	6.84
75.00	0.50	2.00	9.45	5.11	5.54	5.51	7.05	7.09	7.11	7.25	7.49	7.53	7.58	7.72
75.00	0.50	2.50	9.45	4.55	4.97	4.94	6.57	6.61	6.64	6.77	6.90	6.94	6.99	7.13
75.00	0.50	3.00	9.45	4.05	4.44	4.42	6.13	6.17	6.20	6.33	6.39	6.43	6.48	6.62
100.00	0.50	2.00	9.52	5.29	5.69	5.67	7.23	7.27	7.29	7.41	7.65	7.69	7.74	7.89
100.00	0.50	2.50	9.52	4.73	5.13	5.10	6.72	6.76	6.79	6.92	7.06	7.10	7.15	7.29
100.00	0.50	3.00	9.52	4.24	4.62	4.59	6.27	6.32	6.35	6.47	6.55	6.59	6.64	6.78
50.00	0.70	2.00	7.50	3.20	4.48	4.52	6.48	6.51	6.52	6.62	6.75	6.79	6.83	6.95
50.00	0.70	2.50	7.50	2.64	3.96	3.97	5.84	5.86	5.89	5.98	6.04	6.07	6.11	6.20
50.00	0.70	3.00	7.50	2.12	3.44	3.45	5.24	5.26	5.29	5.39	5.41	5.44	5.48	5.57

153 **Table 4 (d)** Web crippling strengths predicted from FEA for CFS channel sections 240×45×15-*t*1.5 with fastened flanges

Bearing length	Elongated web holes		Web crippling strength per web predicted from FEA, P_{FEA}(kN)									
				With edge-stiffened hole								
				Q0.02		Q0.06				Q0.10			
N (mm)	d_w/d_1	b_w/d_w	Plain web	r_q=2 (mm)	r_q=3 (mm)	r_q=2 (mm)	r_q=3 (mm)	r_q=4 (mm)	r_q=6 (mm)	r_q=2 (mm)	r_q=3 (mm)	r_q=4 (mm)	r_q=6 (mm)
50.00	0.30	2.00	8.86	10.66	10.62	10.70	10.66	10.67	10.68	10.71	10.68	10.69	10.68
50.00	0.30	2.50	8.86	10.62	10.59	10.70	10.65	10.67	10.68	10.71	10.65	10.70	10.70
50.00	0.30	3.00	8.86	9.36	9.39	10.10	10.12	10.16	10.19	10.29	10.27	10.26	10.24
75.00	0.30	2.00	10.38	9.41	9.37	10.18	10.18	10.17	10.20	10.35	10.35	10.36	10.40
75.00	0.30	2.50	10.38	8.94	8.93	9.80	9.82	9.78	9.87	10.16	10.18	10.21	10.28
75.00	0.30	3.00	10.38	8.51	8.49	9.43	9.44	9.42	9.50	9.84	9.86	9.89	9.98
100.00	0.30	2.00	11.43	9.82	9.80	10.64	10.65	10.63	10.68	10.92	10.93	10.96	11.02
100.00	0.30	2.50	11.43	9.42	9.39	10.27	10.28	10.26	10.32	10.63	10.64	10.67	10.76
100.00	0.30	3.00	11.43	9.01	9.01	9.91	9.92	9.90	9.97	10.30	10.33	10.36	10.46
50.00	0.50	2.00	8.86	7.91	8.23	9.56	9.65	9.65	9.79	10.11	10.10	10.17	10.27
50.00	0.50	2.50	8.86	8.09	8.40	8.81	8.85	8.87	9.00	9.22	9.22	9.32	9.49
50.00	0.50	3.00	8.86	8.52	8.61	8.33	8.35	8.37	8.42	8.48	8.49	8.52	8.63
75.00	0.50	2.00	10.38	7.38	7.53	9.19	9.23	9.21	9.35	9.62	9.66	9.72	9.88
75.00	0.50	2.50	10.38	7.14	7.22	8.62	8.63	8.58	8.72	8.94	8.97	9.01	9.12
75.00	0.50	3.00	10.38	6.33	6.10	8.01	8.00	8.00	8.08	8.25	8.26	8.25	8.36
100.00	0.50	2.00	11.43	7.87	7.92	9.79	9.84	9.83	9.97	10.19	10.24	10.31	10.47
100.00	0.50	2.50	11.43	7.24	7.40	9.20	9.23	9.23	9.33	9.54	9.57	9.62	9.72
100.00	0.50	3.00	11.43	6.71	6.84	8.59	8.59	8.58	8.69	8.84	8.85	8.87	8.97
50.00	0.70	2.00	8.86	5.94	5.89	8.45	8.48	8.53	8.68	8.56	8.59	8.65	8.79
50.00	0.70	2.50	8.86	5.46	5.49	7.48	7.52	7.59	7.60	7.65	7.68	7.69	7.77
50.00	0.70	3.00	8.86	4.38	3.83	6.57	6.57	6.60	6.58	6.82	6.85	6.88	6.97

154

Table 4 (e) Web crippling strengths predicted from FEA for CFS channel sections 190×45×15 - *t*1.5 with unfastened flanges

Bearing length	Elongated web holes ratio		With edge stiffened holes	Edge-stiffener fillet radius	Web crippling strength	R_{FEA}/R_{P1}
N (mm)	d_w/d_1	b_w/d_w	Q (q/d_1)	r_q (mm)	P_{FEA}(kN)	
50.00	0.7	2	Q0.020	2.00	3.95	0.76
50.00	0.7	2	Q0.020	3.00	3.97	0.76
50.00	0.7	2	Q0.025	2.00	4.89	0.93
50.00	0.7	2	Q0.025	3.00	4.91	0.92
50.00	0.7	2	Q0.030	2.00	5.36	1.00
50.00	0.7	2	Q0.030	3.00	5.41	1.00
50.00	0.7	2	Q0.035	2.00	5.81	1.07
50.00	0.7	2	Q0.035	3.00	5.87	1.07
50.00	0.7	2	Q0.040	2.00	6.20	1.12
50.00	0.7	2	Q0.040	3.00	6.28	1.13
50.00	0.7	2	Q0.045	2.00	6.36	1.14
50.00	0.7	2	Q0.045	3.00	6.42	1.13
50.00	0.7	2	Q0.050	2.00	6.45	1.14
50.00	0.7	2	Q0.050	3.00	6.48	1.13
50.00	0.7	2	Q0.055	2.00	6.49	1.13
50.00	0.7	2	Q0.055	3.00	6.50	1.12
50.00	0.7	2	Q0.060	2.00	6.35	1.09
50.00	0.7	2	Q0.060	3.00	6.41	1.09
50.00	0.7	2	Q0.060	4.00	6.44	1.08
50.00	0.7	2	Q0.060	5.00	6.65	1.11
50.00	0.7	2	Q0.060	6.00	6.63	1.09
50.00	0.7	2	Q0.060	7.00	6.80	1.11
50.00	0.7	2	Q0.060	8.00	6.87	1.11
50.00	0.7	2	Q0.060	9.00	6.94	1.11
50.00	0.7	2	Q0.060	10.00	7.00	1.11
50.00	0.7	2	Q0.060	11.00	7.05	1.11

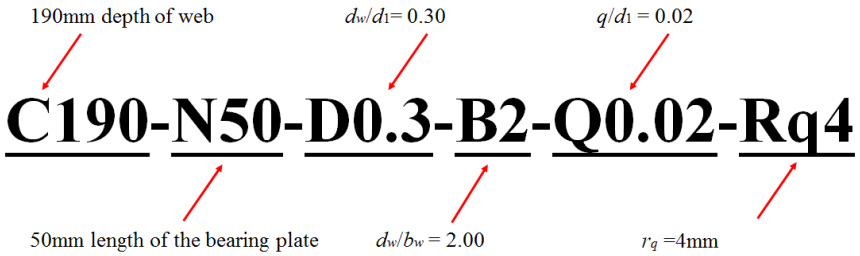

Fig. 12 Specimen labelling for a parametric study

3.1 Effects of d_w/d_1 and r_q/t on the web crippling strength reduction factor

The effect of d_w/d_1 on the web crippling strength reduction factor is shown in Fig. 13. A decrease in the strength reduction factor for the channel sections C190-N50-B2 was observed, when the values of d_w/d_1 increased from 0.3 to 0.7. It can be seen from Fig. 13 that

the d_w/d_1 has a considerable influence on the web crippling strength reduction factor, particularly for specimens with the smaller edge-stiffener length ratio (i.e., Q0.02) and smaller edge-stiffener fillet radius (i.e., Rq2). From Fig. 13, it can be seen that the web crippling strength reduction factor of CFS channel sections with fastened flanges was higher than those with unfastened flanges.

The effect of r_q/t on the web crippling strength reduction factor was shown in Fig. 14. It can be seen from Fig. 14 that the values of the web crippling strength reduction factor for the channel sections C190-N50-D0.3 have a slight increase when the r_q/t increased from 1.33 to 4.00.

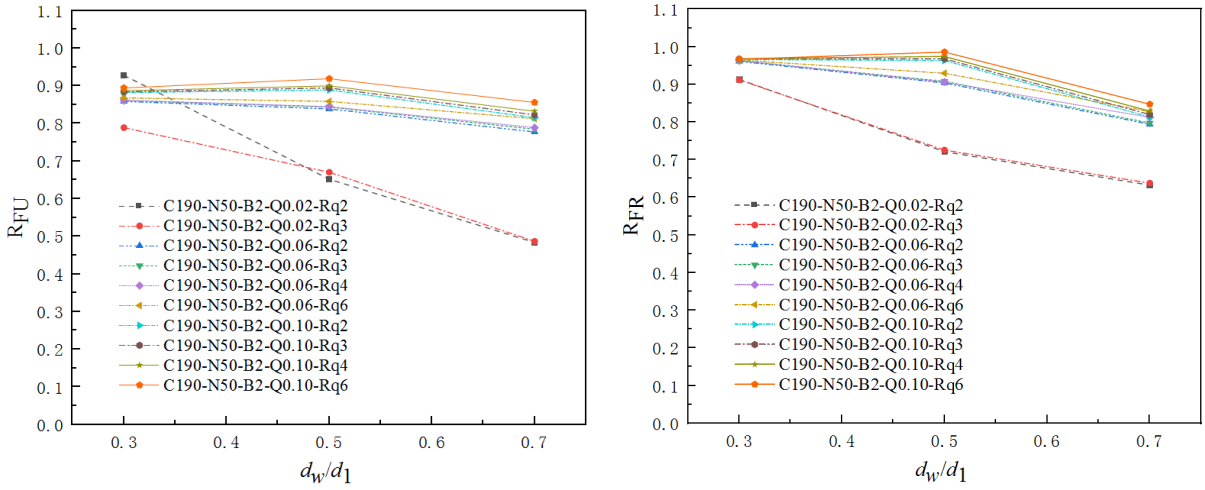

(a) Unfastened flanges (b) Fastened flanges

Fig. 13 Variation in reduction factor with d_w/d_1 for C190-N50-B2

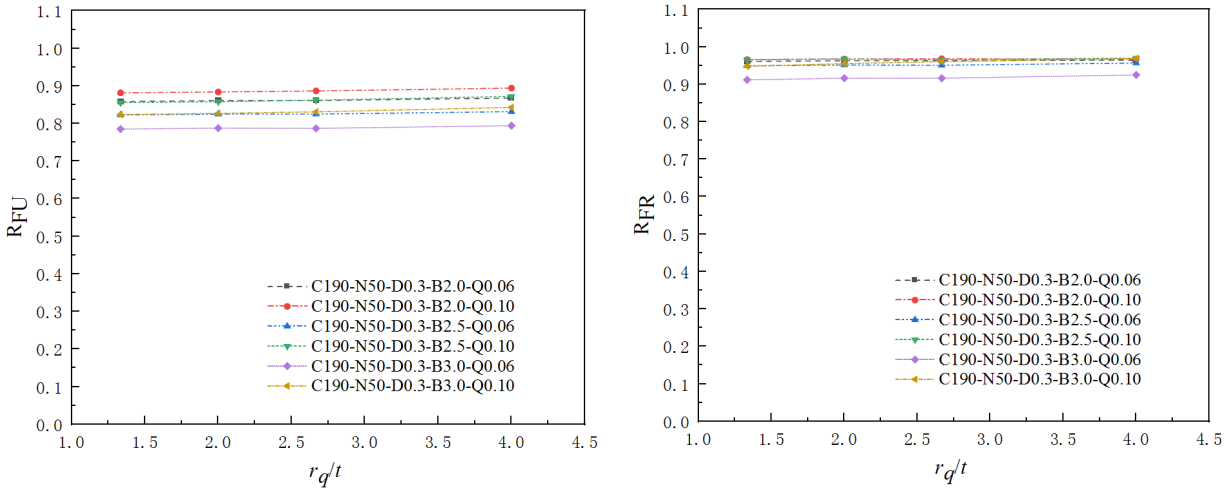

(a) Unfastened flanges (b) Fastened flanges

Fig. 14 Variation in reduction factor with r_q/t for C190-N50-D0.3

3.2 Effects of b_w/d_w, N/d_1 and q/d_1 on the web crippling strength reduction factor

The web crippling strength from the parametric study was summarized in Table 4. The effects of the d_w/b_w, N/d_1, and q/d_1 on the web crippling strength reduction factor were shown in Figs. 15, 16, and 17, respectively. In Fig. 15, for the channel sections C190-N50-Rq2, when the d_w/b_w increased from 2.00 to 3.00, the web crippling reduction factor showed a downward trend with different q/d_1 and d_w/d_1, especially for those specimens with unfastened flanges. Compared to CFS sections with a plain web, for the case of an elongated un-stiffened web hole, the average reduction for sections with an aspect ratio of two and three in web crippling strength was 39% and 49%, respectively. However, for an elongated edge-stiffened hole, the reduction in the web crippling strength was reduced to only 2% and 16%, respectively. It can be seen from Fig. 16 that the variation of N/d_1 has a slight effect on the web crippling strength reduction factor of the channel sections C190-Q0.02-Rq2.

The effect of the q/d_1 on the web crippling strength reduction factor was shown in Fig. 17. It is important to note that for the channel sections C190-N50-Rq2, q/d_1 had a significant

effect on the web crippling strength reduction factor, especially for those specimens with a large aspect ratio (i.e., B3.0) and a large ratio of the width of the hole to the depth of the web (i.e., D0.7). For instance, the strength reduction factor of channel sections C190-N50-D0.7-B3.0-Rq2 with unfastened flanges increased from 0.37 to 0.65 when the ratio q/d_1 increased from 0.02 to 0.10, and the same increasing trend was noticed for the channel sections C190-N50-D0.7-B3.0-Rq2 with fastened flanges. From the FEA results, it was found that out of the five parameters, the edge-stiffener length ratio (q/d_1) has the most significant effect on the web crippling strength of CFS channel sections.

The relationship between the web crippling strength reduction factor and the edge-stiffener length ratio Q (q/d_1) is depicted in Fig. 18. When the edge-stiffener length ratio increased from 0.02 to 0.10, the value of the web crippling strength reduction factor increasingly approached to 1, further demonstrating the significant effect of Q on the web crippling strength of CFS channel sections having elongated edge-stiffened web holes.

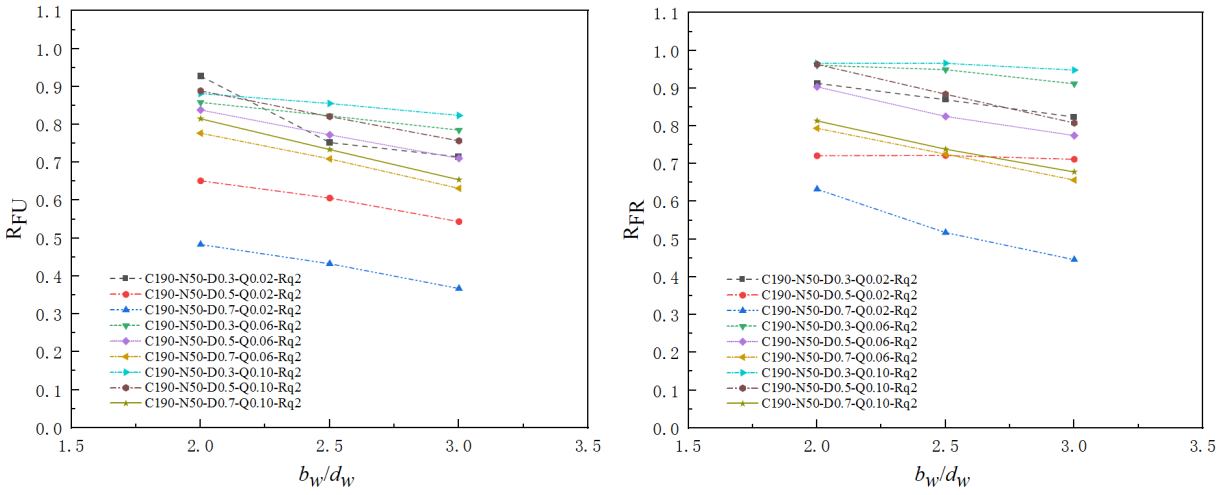

(a) Unfastened flanges (b) Fastened flanges

Fig. 15 Variation in reduction factor with b_w/d_w for C190-N50-Rq2

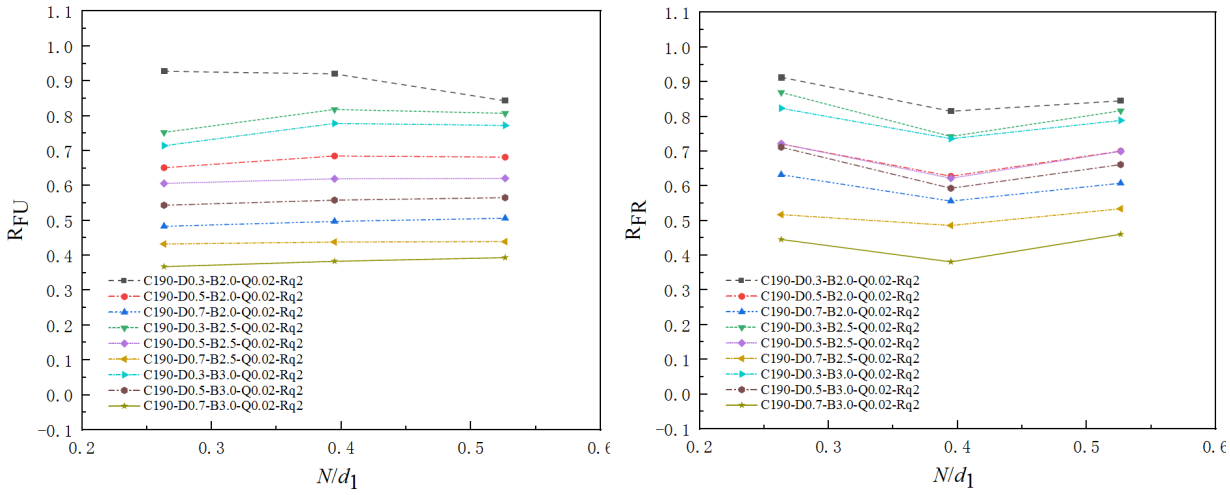

(a) Unfastened flanges (b) Fastened flanges

Fig. 16 Variation in reduction factor with N/d_1 for C190-Q0.02-Rq2

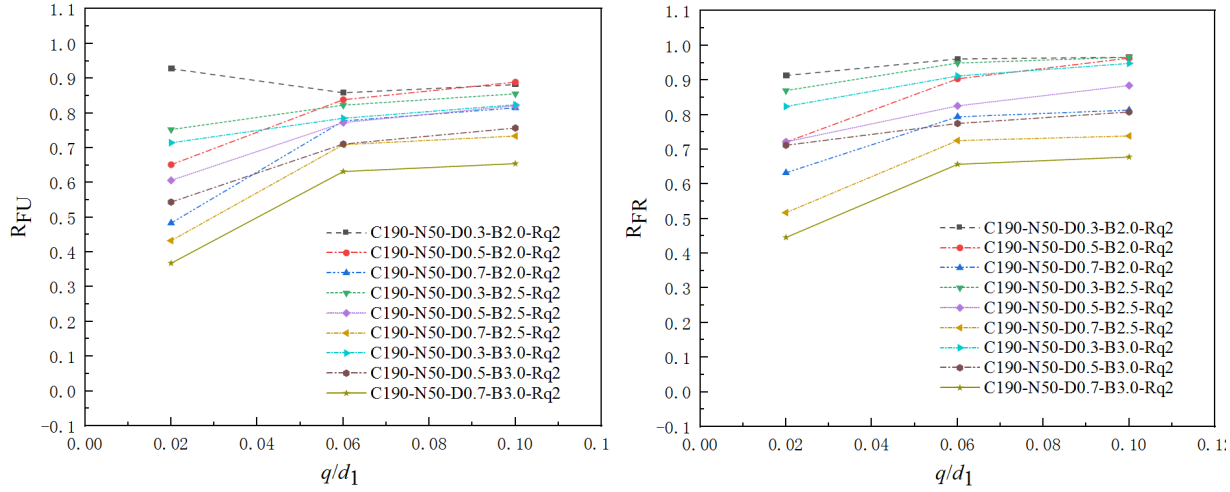

(a) Unfastened flanges (b) Fastened flanges

Fig. 17 Variation in reduction factor with q/d_1 for C190-N50-Rq2

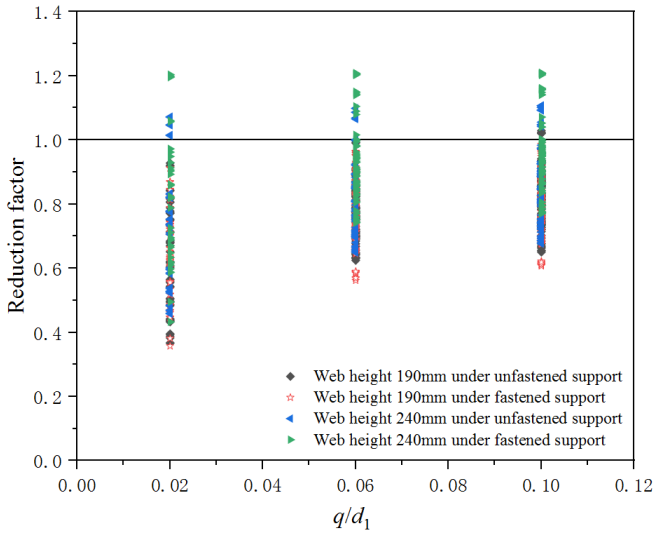

Fig.18 Variation in reduction factors with q/d_1

4 Proposed web crippling design equations

4.1 Proposed web crippling strength reduction factor equations

Evaluation of the numerical simulation results revealed that the d_w/d_1, b_w/d_w, r_q/t, N/d_1, and q/d_1 were the main parameters that affected the web crippling strength reduction factors of the channel sections having elongated edge-stiffened holes. Regression analysis was performed using Origin Lab [22] to develop the equations for web crippling strength reduction factors (R_P). The web crippling strength reduction factor equations were proposed as follows:

For the CFS channel sections with unfastened flanges,

$$R_{P1} = 1.13 - 0.41\left(\frac{d_w}{d_1}\right) - 0.11\left(\frac{b_w}{d_w}\right) - 0.16\left(\frac{N}{d_1}\right) + 0.01\left(\frac{r_q}{t}\right) + 2.04\left(\frac{q}{d_1}\right) \le 1 \quad (4)$$

For the CFS channel sections with fastened flanges,

$$R_{P2} = 1.32 - 0.51\left(\frac{d_w}{d_1}\right) - 0.10\left(\frac{b_w}{d_w}\right) - 0.44\left(\frac{N}{d_1}\right) + 0.01\left(\frac{r_q}{t}\right) + 1.66\left(\frac{q}{d_1}\right) \le 1 \quad (5)$$

By calculating R_{FEA}/R_{P1} and R_{FEA}/R_{P2} (see Fig. 19), it was found that the values of the web crippling strength reduction factor were much larger than or much less than 1 when Q is 0.02, which means Eqs. (4) and (5) were no longer applicable. In order to accurately determine the range of application of the Eqs. (4) and (5), the effects of q and r_q on R_{FEA}/R_{P1} and R_{FEA}/R_{P2} were investigated in Table 4 (e), and it was found that the proposed equations were unreliable to predict the web crippling strength reduction factor when q/d_1 was less than 0.025. Overall, the limitations for the proposed equations (Eqs. (4) and (5)) are: $0.025 \le q/d_1$

215 ≤ 0.10, $0.30 \leq d_w/d_1 \leq 0.70$, $0.27 \leq N/d_1 \leq 0.54$, 2 mm $\leq r_q \leq$ 6 mm, $2.00 \leq b_w/d_w \leq 3.00$ and θ

216 $= 90°$.

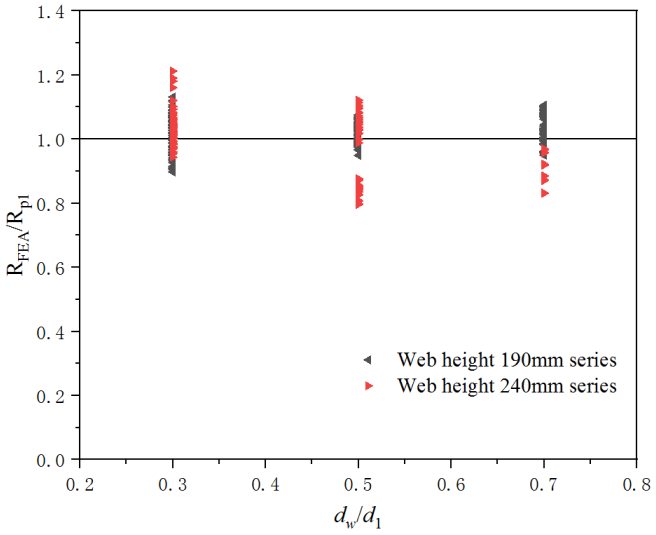

(a) Unfastened flanges

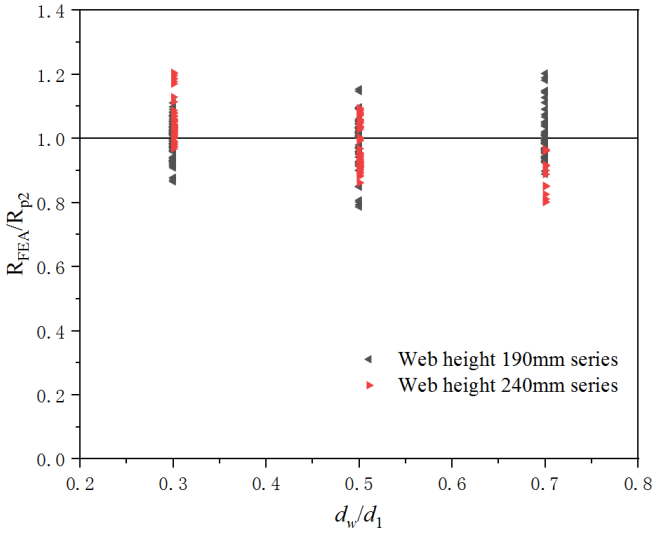

(b) Fastened flanges

Fig. 19 Comparison of reduction factors

217 *4.2 Proposed DSM-based equations*

218 The application of web crippling strength reduction factor equations was limited to

219 some specific CFS channel sections and did not consider the effects of r_i, b_f and f_y. DSM

220 provides an alternative approach to predicting the web crippling strength of CFS channel

221 sections, and is more general as its covers all the buckling modes in one method. The
222 previous studies on the application of DSM mainly investigated the web crippling behaviour
223 of CFS plain channel sections. However, the investigation procedure can be adopted in the
224 current study to explore the effects of elongated edge-stiffened web holes on the web
225 crippling behaviour of CFS channel sections. Several researchers [23-28] have proposed
226 DSM-based web crippling design equations using a format of Eq. (6) for CFS plain channel
227 sections under different loading conditions.

228 $$P_b = n_3 P_{b,y}\left[1 - n_1\left(\frac{P_{b,cr}}{P_{b,y}}\right)^{n_2}\right]\left(\frac{P_{b,cr}}{P_{b,y}}\right)^{n_2} \quad (6)$$

229 The critical buckling load ($P_{b,cr}$) and the yield load ($P_{b,y}$) were two key parameters in
230 Eq. (6). Sundararajah et al. [4, 29-33] and Sundararajah [34] proposed DSM-based equations
231 to predict the web crippling capacities of CFS plain channel sections, and they determined the
232 $P_{b,cr}$ using elastic buckling FEA and the $P_{b,y}$ using idealized failure mechanisms based on the
233 deformed shapes observed in experiments and FEA.

234 *4.2.1 Critical buckling load ($P_{b,cr}$)*

235 The critical buckling loads of CFS channel sections with unfastened flanges were
236 derived from linear buckling analyses [34] using ABAQUS [21]. The nodal forces were used
237 to simulate the load at the junction between the web and the flange. The boundary conditions
238 were shown in Fig. 20, and further details could be found in the literature [34]. FE models
239 were developed to obtain the elastic critical buckling loads ($P_{b,cr}$) of CFS channel sections
240 having elongated un-stiffened and edge-stiffened web holes under the unfastened flange

condition, and the details of such specimens were shown in the Appendix. $P_{b,cr}$ were used to calculate the buckling coefficient (k_{FEA}) using Eq. (7).

$$P_{b,cr} = \frac{\pi^2 Ekt^3}{12(1-\nu^2)d_1} \tag{7}$$

where E represents the elastic modulus of steel, k represents the critical buckling coefficient, t represents the section thickness, ν represents the poisson's ratio, and d_1 represents the clear height of web.

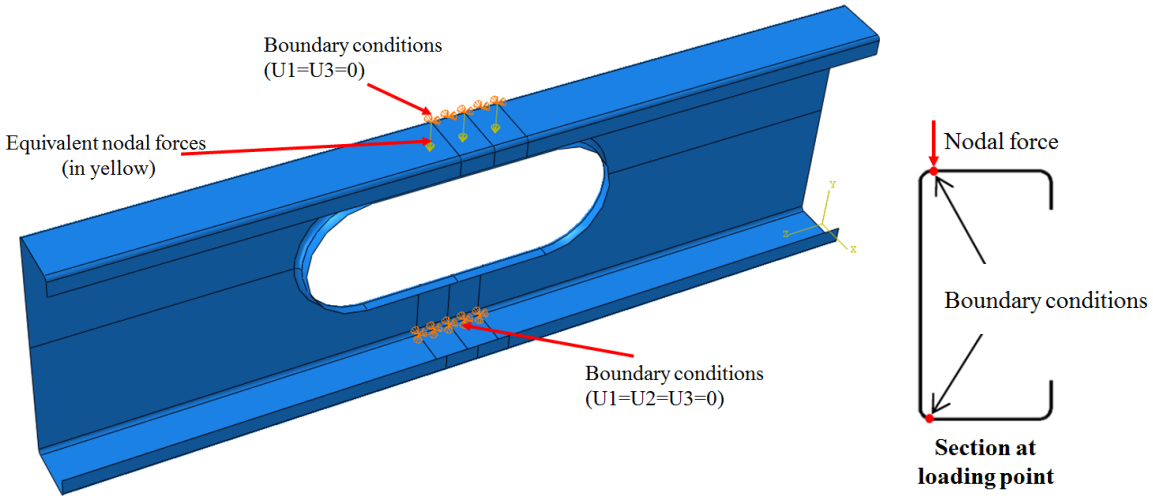

Fig. 20 Elastic buckling analysis of CFS channel sections under ITF load case

An equation considering the effects of elongated un-stiffened and edge-stiffened web holes on the web crippling strength of CFS channel sections was proposed with nine different coefficients linking the eight key parameters in the form of Eq. (8) to calculate k_{prop}. The values of such coefficients were obtained based on nonlinear regression analysis using Origin Lab [22], and were shown in Table 5. As can be seen, the mean values of k_{FEA}/k_{prop} were 0.97 and 1.01, with corresponding COVs of 0.14 and 0.13.

$$k = C\left(1+C_1\sqrt{\frac{r_i}{t}}\right)\left(1+C_2\sqrt{\frac{d_1}{t}}\right)\left(1+C_3\sqrt{\frac{N}{t}}\right)\left(1+C_4\sqrt{\frac{b_f}{t}}\right)\left(1+C_5\sqrt{\frac{d_w}{t}}\right)\left(1+C_6\sqrt{\frac{b_w}{t}}\right)\left(1+C_7\sqrt{\frac{r_q}{t}}\right)\left(1+C_8\sqrt{\frac{q}{t}}\right) \quad (8)$$

where C represents the general coefficient, C_1, C_2, C_3, C_4, C_5, C_6, C_7 and C_8 were the coefficients of inside fillet radius of section to thickness ratio, web slenderness ratio, bearing length to thickness ratio, flange width to thickness ratio, width of the elongated web holes to thickness ratio, length of the elongated web holes to thickness ratio, inside fillet radius between web and hole edge-stiffener to thickness ratio and length of edge-stiffener to thickness ratio, respectively.

Table 5 Proposed coefficients for buckling coefficient equations

Elongated web holes	C	C_1	C_2	C_3	C_4	C_5	C_6	C_7	C_8	Mean	COV
Un-stiffened	-3.47	0.25	-0.15	0.06	0.07	-0.05	-0.04	0	0	0.97	0.14
Edge-stiffened	0.24	-0.30	-0.16	0.08	-3.25	0.07	-0.04	-0.01	0.03	1.01	0.13

4.2.2 Yield load ($P_{b,y}$)

Yield load ($P_{b,y}$) determination is difficult due to the complicated web crippling failure. Different approaches used by past studies [24-27, 35] have been mainly based on post-failure yield line mechanisms observed from experiments and/or FEA. Using the Principle of Virtual Work, they [26, 27] proposed a predictive equation in the form of Eq. (9) for the $P_{b,y}$ using idealized plastic mechanisms for the case of unfastened flanges. For the CFS channel sections having elongated un-stiffened web holes, the main yield line in the web reaches both edges of sections when the web crippling strength reaches its maximum value (see Fig. 21(a)). Based on this observation, the yield line dimension (N_{m1}) was assumed equal to the section length (L) minus the length of elongated web holes. For the CFS channel sections having elongated

edge-stiffened web holes, the failure mode is shown in Fig. 21(b), and the web yield line does not appear to reach the beam edges based on the Mises stress distribution. In this case, the main yield line appeared in the edge-stiffener, and the yield line dimension (N_{m2}) was defined based on the specific failure mode. Eqs. (10) and (11) were proposed to calculate N_m for CFS channel sections having elongated un-stiffened and edge-stiffened web holes under the ITF loading condition based on the parametric study in the current study, and the simplified yield mechanisms for the typical ultimate failure modes were shown in Fig. 21.

$$P_{b,y} = f_y N_m \left(\sqrt{4r_m^2 + t^2} - 2r_m \right) \tag{9}$$

For CFS channel sections having an un-stiffened web hole,

$$N_{m1} = L - b_w \tag{10}$$

For CFS channel sections having an edge-stiffened web hole,

$$N_{m2} = \pi d_w \tag{11}$$

where r_m represents the inside fillet radius from the mid-thickness line ($r_m = r_i + t/2$).

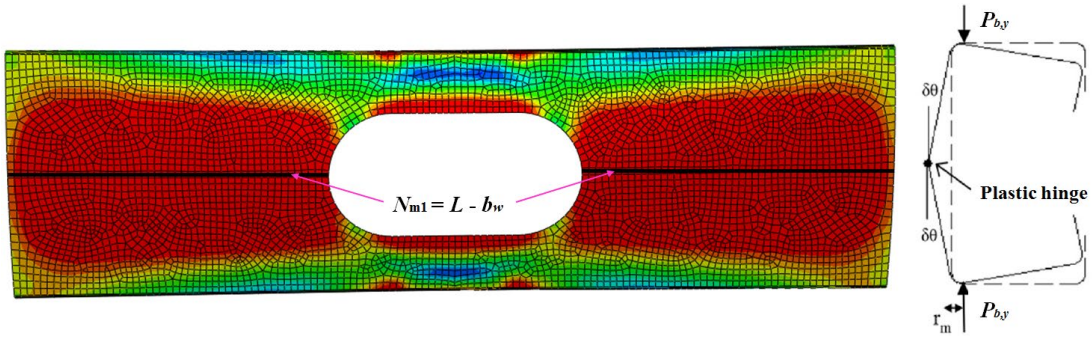

(a) Un-stiffened (C190-N100-D0.3-B2, t=1.5mm & f_y = 288 MPa)

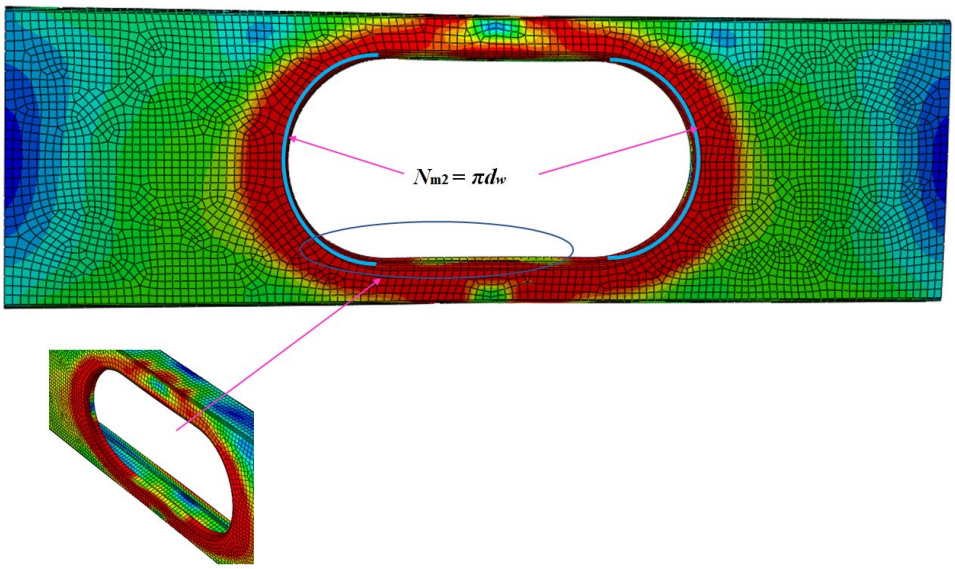

(b) Edge-stiffened (C190-N50-D0.7-B2-Q0.06-Rq5, t=1.5mm & f_y = 288 MPa)

Fig. 21 Yield mechanism length

4.2.3 DSM-based equation

In the past, Eq. (6) with three factors (n_1, n_2 and n_3) was used [23, 26-27] to calculate the web crippling strength. However, the standard DSM equation was based on the condition when n_3 is equal 1 [36]. In the current study, an unified DSM-based equation were proposed for CFS channel sections having elongated un-stiffened and edge-stiffened web holes under the unfastened flanges to predict the ITF web crippling strength. The ITF web crippling strengths (P_b) were obtained from the parametric study. The buckling loads ($P_{b,cr}$) were calculated by Eqs. (7) and (8) based on linear buckling analyses, and the yield loads ($P_{b,y}$) were calculated by Eqs. (9), (10) or (11). The suitable coefficients n_1 and n_2 need to be determined for the Eqs. (12) and (13). Using Origin Lab [22], a regression analysis was performed to obtain such coefficients based on the results of the parametric study, and the DSM-based equations were then proposed. The comparison of web crippling capacities of CFS specimens from the parametric study with the proposed DSM-based equation in this

297 paper was shown in Fig. 22. It should be mentioned that Eqs. (12) and (13) did not consider
298 pure yielding (web yielding or flange crushing) failure modes (Region-A) because it is
299 difficult to precisely define the limits.

300 For $\lambda \le 0.938$, $P_b = P_{b,y}$ (12)

301 For $\lambda > 0.938$, $\frac{P_b}{P_{b,y}} = \left[1 - 0.11\left(\frac{P_{b,cr}}{P_{b,y}}\right)^{1.07}\right]\left(\frac{P_{b,cr}}{P_{b,y}}\right)^{1.07}$ (13)

302 $\lambda = \sqrt{\frac{P_{b,y}}{P_{b,cr}}}$ (14)

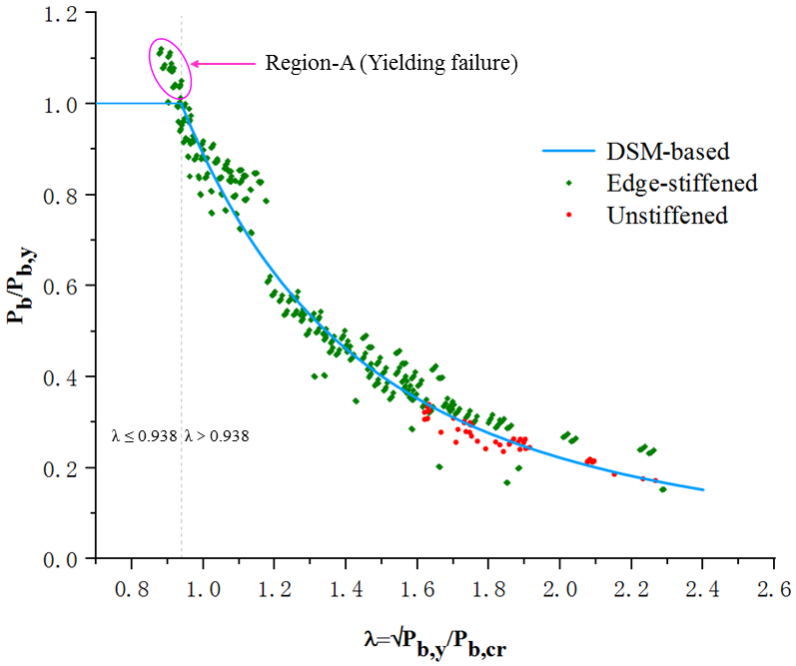

Fig. 22 Comparison of web crippling strength of CFS specimens from a parametric study with proposed DSM-based equations

303 *4.3 Comparison of the numerical results with the proposed equations*

304 Table 6 showed the results of comparing the web crippling strength determined from
305 proposed equations and the parametric study. The findings from Table 6 show that the ratio

306 P_{FEA}/P_{RP1} is 1.05 with a COV of 0.10, and the ratio P_{FEA}/P_b is 1.00 with a COV of 0.06. The

307 DSM-based equation shows less variability compared to another equation.

308 **Table 6** Comparison of FEA results with proposed equations

Specimen	P_{FEA}	For web crippling strength reduction factor equation				For DSM-based equation	
		$P_{FEA,\ plain}$	R_{p1}	P_{RP1}	P_{FEA}/P_{RP1}	P_b	P_{FEA}/P_b
	(kN)	(kN)		(kN)		(kN)	
C190-N50-D0.3-B2.0-Q0.06-Rq3	7.03	8.16	0.86	7.02	1.00	7.55	0.93
C190-N50-D0.3-B2.0-Q0.06-Rq6	7.08	8.16	0.91	7.43	0.95	7.49	0.94
C190-N50-D0.3-B2.0-Q0.10-Rq3	7.22	8.16	0.97	7.92	0.91	7.71	0.94
C190-N50-D0.3-B2.0-Q0.10-Rq6	7.30	8.16	1.00	8.16	0.89	7.65	0.95
C190-N50-D0.3-B2.5-Q0.06-Rq3	6.74	8.16	0.83	6.77	1.00	7.12	0.95
C190-N50-D0.3-B3.0-Q0.06-Rq3	6.43	8.16	0.80	6.53	0.98	6.73	0.96
C190-N50-D0.5-B2.0-Q0.06-Rq3	6.89	8.16	0.81	6.61	1.04	7.11	0.97
C190-N50-D0.7-B2.0-Q0.06-Rq3	6.41	8.16	0.73	5.96	1.08	6.43	1.00
C190-N75-D0.3-B2.0-Q0.06-Rq3	8.21	8.28	0.87	7.20	1.14	8.06	1.02
C190-N100-D0.3-B2.0-Q0.06-Rq3	8.27	9.12	0.85	7.75	1.07	8.48	0.98
C240-N50-D0.3-B2.0-Q0.06-Rq3	8.24	7.50	0.90	6.75	1.22	7.54	1.09
C240-N50-D0.3-B2.0-Q0.06-Rq6	8.24	7.50	0.92	6.90	1.19	7.48	1.10
C240-N50-D0.3-B2.0-Q0.10-Rq3	8.30	7.50	0.98	7.35	1.13	7.70	1.07
C240-N50-D0.3-B2.0-Q0.10-Rq6	8.31	7.50	1.00	7.50	1.11	7.64	1.08
Mean					1.05		1.00
COV					0.10		0.06

Note：$P_{FEA,\ plain}$ represents the numerical results of web crippling strength for CFS plain channel sections, and the P_{RP1} represents the web crippling strength calculated by multiplying the $P_{FEA,\ plain}$ and R_{P1}.

309 # 5 Reliability analysis

310 A reliability analysis was carried out to evaluate the reliability of the proposed design

311 equations in the form of web crippling reduction factor (R_p) and a DSM-based equation for

312 CFS sections with elongated web holes. The reliability index (β) is a relative indicator of the

313 design's safety, and AISI S100-16 [11] recommends a reliability index of 2.5 for CFS

314 structural members. The design equations are considered dependable if the reliability index

(β) is greater than or equal to 2.50. For the CFS structural members, the reliability index (β) could be determined using Eq. (15).

$$\phi = 1.52\left(M_m F_m P_m\right) e^{-\beta\sqrt{V_M^2 + V_F^2 + C_P V_P^2 + V_Q^2}} \quad (15)$$

$$C_P = \left[1 + \frac{1}{n}\right]\left[\frac{m}{m-2}\right] \quad (16)$$

where M_m and V_M = mean values (1.10) and coefficient of variation (COV) (0.1) of the material properties. F_m and V_F = mean values (1.00) and COV (0.05) of the fabrication factor. The statistical parameters P_m and V_P represent the load ratio's mean value and COV, respectively. V_Q = COV (0.21) of the load effect. A constant resistance factor (ϕ) of 0.85 [1] was used in the reliability analysis. The correction factor (C_P) could be determined by Eq. (16), and n and m are the number of specimens and degree of freedom ($m = n - 1$), respectively.

Table 7 Statistical analysis for comparison of web crippling strength reduction factor for specimens with unfastened flanges

Statistical parameters	R[FEA]/R_{p1}[1.13-0.41 $\left(\frac{d_w}{d_1}\right)$ -0.11 $\left(\frac{b_w}{d_w}\right)$ -0.16 $\left(\frac{N}{d_1}\right)$ +0.01 $\left(\frac{r_q}{t}\right)$ +2.04($\frac{q}{d_1}$)]
Mean, P_m	1.010
Coefficient of variation, V_P	0.070
Reliability index, β	2.532
Resistance factor, ϕ	0.850

Table 8 Statistical analysis for comparison of web crippling strength reduction factor for specimens with fastened flanges

Statistical parameters	R[FEA]/R_{p2}[1.32-0.51 $\left(\frac{d_w}{d_1}\right)$ -0.10 $\left(\frac{b_w}{d_w}\right)$ -0.44 $\left(\frac{N}{d_1}\right)$ +0.01 $\left(\frac{r_q}{t}\right)$ +1.66($\frac{q}{d_1}$)]
Mean, P_m	1.013
Coefficient of variation, V_P	0.071
Reliability index, β	2.545
Resistance factor, ϕ	0.850

Table 9 Statistical analysis for comparison of web crippling strength for CFS channel sections having elongated un-stiffened and edge-stiffened web holes

Statistical parameters	P_b[FEA]/$P_{b,\mathrm{DSM}}$[$P_{b,y}$(1-0.11($P_{b,cr}$/$P_{b,y}$)^1.07)($P_{b,cr}$/$P_{b,y}$)^1.07]	
	Un-stiffened web holes	Edge-stiffened web holes
Mean, P_m	1.012	1.030
Coefficient of variation, V_P	0.062	0.094
Reliability index, β	2.639	2.520
Resistance factor, ϕ	0.850	0.850

5.1 Reliability analysis for web crippling strength reduction factor equations

The values of the web crippling strength reduction factor R_FEA obtained from the results of the parametric study were compared with the values of the proposed web crippling strength reduction factors R_{P1} and R_{P2} calculated using Eqs. (4) and (5), as shown in Fig. 19. The values of the web crippling strength reduction factor calculated based on equations were generally conservative and agree well with the numerical results. Tables 7 and 8 summarize the results of a reliability analysis. As can be seen from Tables 7 and 8, the mean values of the web crippling reduction factor ratios were 1.010 and 1.013, with the corresponding COV of 0.070 and 0.071, and reliability indices (β) of 2.53 and 2.55 for the specimens with unfastened and fastened flanges, respectively. As a result, the reliability index (β) was higher than the desired value of 2.5, and the two proposed equations could be used to predict web crippling strength reduction factors of the CFS channel sections having elongated edge-stiffened web holes under the ITF loading condition.

5.2 Reliability analysis for DSM-based equation

The values of the web crippling strength $P_{b,\mathrm{FEA}}$ obtained from the results of the parametric study were compared with the values of the web crippling strength calculated using proposed DSM-based equation, as shown in Fig. 21. The results of reliability analysis

were summarized in Tables 9, and the mean values of the $P_{b,\mathrm{FEA}}/P_{b,\mathrm{DSM}}$ were 1.01 and 1.03, with the corresponding COVs of 0.06 and 0.09, and reliability indices (β) of 2.64 and 2.52 for the CFS channel sections having elongated un-stiffened and edge-stiffened web holes, respectively. The reliability of all the proposed DSM-based equations was demonstrated by means of statistical analyses, showing their suitability for incorporation into future revisions of international design codes for CFS structures.

6 Conclusions

This paper presents a numerical study to investigate the web crippling behaviour of CFS channel sections having elongated un-stiffened and edge-stiffened web holes under interior-two-flange (ITF) loading condition. The developed FE models were validated against the experimental results reported by Chen et al. (2021), which showed good agreement in terms of the load-displacement curves and deformed shapes. A total of 1,227 finite element analysis results were reported. The effects of unfastened and fastened flanges, q/d_1, d_w/d_1, d_w/b_w, N/d_1 and r_q/t ratio on the web crippling strength of CFS channel sections were investigated. The following conclusions can be drawn:

(1) According to results of the parametric study, the q/d_1, d_w/d_1, and d_w/b_w have a large influence on the web crippling strength reduction factor.

(2) The design equations for the web crippling strength reduction factor of CFS channel sections having elongated edge-stiffened web holes were proposed based on linear regression analysis. The limits of the proposed equations were $0.025 \le q/d_1 \le 0.10$, $0.30 \le d_w/d_1 \le 0.70$, $0.27 \le N/d_1 \le 0.54$, 2 mm $\le r_q \le$ 6 mm, $2.00 \le b_w/d_w \le 3.00$ and $\theta = 90°$. A

comprehensive reliability analysis was performed, which showed that the proposed equations could be used to accurately calculate the web crippling strength reduction factor of CFS channel sections having elongated edge-stiffened web holes under the ITF loading condition.

(3) A unified DSM-based equation was proposed for CFS channel sections having elongated un-stiffened and edge-stiffened web holes under the unfastened flange condition to determine the ITF web crippling strength. Finally, a reliability analysis was conducted to show that the unified DSM-based equation is reliable.

Acknowledgement

The authors appreciate the use of the high-performance computer at the University of Waikato.

References

[1] A. Uzzaman, J.B.P. Lim, D. Nash, K. Roy, Web crippling behaviour of cold-formed steel channel sections with edge-stiffened and un-stiffened circular holes under interior-two-flange loading condition, Thin-Walled Structures. 154 (2020) 106813.

[2] B. Chen, K. Roy, Z. Fang, A. Uzzaman, Y. Chi, J. B. P. Lim, (2021). Web crippling capacity of fastened cold-formed steel channel sections with edge-stiffened web holes, un-stiffened web holes and plain webs under two-flange loading, Thin-Walled Structures, 163, 107666.

[3] L. Sundararajah, M. Mahendran, P. Keerthan, (2016). Experimental Studies of Lipped Channel Beams Subject to Web Crippling under Two-Flange Load Cases. Journal of Structural Engineering (New York, N.Y.), 142(9).

[4] Howick Floor, Joist System, 2013. Auckland, New Zealand.

[5] K. Roy, C. Mohammadjani, J. B. P. Lim, (2019). Experimental and numerical investigation into the behaviour of face-to-face built-up cold-formed steel channel sections under compression. Thin-Walled Structures, 134, 291–309.

[6] B. Chen, K. Roy, A. Uzzaman, G. M. Raftery, D. Nash, G. C. Clifton, P. Pouladi, J. B. P. Lim, (2019). Effects of edge-stiffened web openings on the behaviour of cold-formed steel channel sections under compression. Thin-Walled Structures, 144, 106307–. https://doi.org/10.1016/j.tws.2019.106307

394 [7] B. Chen, K. Roy, A. Uzzaman, J.B.P. Lim, Moment capacity of cold-formed channel
395 beams with edge-stiffened web holes, un-stiffened web holes and plain webs,
396 Thin-Walled Structures, 157.
397 [8] B. Chen, K. Roy, A. Uzzaman, J. B. P. Lim, (2020). Moment capacity of cold-formed
398 channel beams with edge-stiffened web holes, un-stiffened web holes and plain webs.
399 Thin-Walled Structures, 157, 107070–. https://doi.org/10.1016/j.tws.2020.107070
400 [9] P. Gatheeshgar, K. Poologanathan, S. Gunalan, C. Dimopoulos, G. Vasdravellis, (2023).
401 Elastic shear buckling of cold-formed steel channels with edge stiffened web holes.
402 Thin-Walled Structures, 185, 110551–. https://doi.org/10.1016/j.tws.2023.110551
403 [10] B. Chen, K. Roy, Z. Fang, A. Uzzaman, C. H. Pham, G. M. Raftery, J. B. P. Lim,
404 (2022). Shear capacity of cold-formed steel channels with edge-Stiffened web holes,
405 unstiffened web holes, and plain webs. Journal of Structural Engineering (New York,
406 N.Y.), 148(2). https://doi.org/10.1061/(ASCE)ST.1943-541X.0003250
407 [11] AISI (American Iron and Steel Institute). 2016. North American specification for the
408 design of cold-formed steel structural members. AISI S100-16. Washington, DC: AISI.
409 [12] AS/NZS (Australian/New Zealand Standard) 2018. Cold-formed steel structures.
410 AS/NZS 4600:2018. Sydney, Australia: Standards Australia.
411 [13] Euro code 3 Part 1.3 (ECS), Design of Steel Structures: Part 1.3: General
412 Rules-Supplementary Rules for Cold-Formed Thin Gauge Members and Sheeting,
413 European Committee for Standardization, Brussels, Belgium, 2006.

414 [14] Y. Lian, A. Uzzaman, J.B.P. Lim, G. Abdelal, D. Nash, B. Young, Effect of web holes
415 on web crippling strength of cold-formed steel channel sections under end-one-flange
416 loading condition - Part II: parametric study and proposed design equations,
417 Thin-Walled Structures. 107 (2016) 489–501.
418 [15] Y. Lian, A. Uzzaman, J.B.P. Lim, G. Abdelal, D. Nash, B. Young, Web crippling
419 behaviour of cold-formed steel channel sections with web holes subjected to
420 interior-one-flange loading condition – Part II: parametric study and proposed design
421 equations, Thin-Walled Structures. 114 (2017) 92–106.
422 [16] A. Uzzaman, J.B.P. Lim, D. Nash. J. Rhodes, B. Young, Cold-formed steel sections with
423 web openings subjected to web crippling under two-flange loading conditions-Part II:
424 Parametric study and proposed design equations, Thin-Walled Structures. 56, 79-87.
425 [17] R.A. LaBoube, W.W. Yu, S.U. Deshmukh, C.A. Uphoff. Crippling capacity of web
426 elements with openings, Struct. Eng. 125 (1999) 137-141.
427 [18] R.A. LaBoube, W.W. Yu, J.E. Langan, Cold-formed steel web with openings: summary
428 report, Thin-Walled Structures. 28 (1997) 355-372.
429 [19] K.F. Chung, Structural performance of cold-formed sections with single and multiple
430 web openings, Part-1: experimental investigation 73, The Structural Engineer, 1995.
431 [20] K.F. Chung, Structural performance of cold-formed sections with single and multiple
432 web openings, Part-2: design rules 73, The Structural Engineer, 1995.
433 [21] ABAQUS Analysis User's Manual-Version 6.14-2, ABAQUS Inc., USA, 2018.
434 [22] Origin Lab (Version 8.5.1). Origin Lab Corporation, Northampton, MA, USA

435 [23] A.P.C. Duarte, N.M. Silvestre, A new slenderness-based approach for the web crippling
436 design of plain channel steel beams, International Journal of Steel Structures 13 (2014)
437 421–434.
438 [24] M.Y. Choy, X.F. Jia, X. Yuan, J. Zhou, H.S. Wang, C. Yu, Direct Strength Method for
439 Web Crippling of Cold-Formed Steel C- and Z-Sections Subjected to Two-Flange
440 Loading, Annual Stability Conference of Structural Stability Research Council, Toronto,
441 Canada, 2014, pp. 99-111.
442 [25] P. Keerthan, M. Mahendran, E. Steau, Experimental study of web crippling behavior of
443 hollow flange channel beams under two flange load cases, Thin-Walled Structures.
444 85(2) (2014) 207–219.
445 [26] P. Natário, N. Silvestre, D. Camotim, Direct strength prediction of web crippling failure
446 of beams under ETF loading, Thin-Walled Structures. 98 (2016) 360–374.
447 [27] P. Natário, N. Silvestre, D. Camotim, Web crippling of beams under ITF loading: a
448 novel DSM-based design approach, J. Constr. Steel Res. 128 (2017) 812–824.
449 [28] V.V. Nguyen, G.J. Hancock, C.H. Pham, New developments in the direct strength
450 method (DSM) for the design of cold-formed steel sections under localised loading,
451 Steel Construction 10 (3) (2017) 227–233.
452 [29] L. Sundararajah, M. Mahendran, P. Keerthan, Web crippling experiments of high
453 strength lipped channel beams under one-flange loading, J. Constr. Steel Res. 138
454 (2017) 851–866.

455 [30] L. Sundararajah, M. Mahendran, P. Keerthan, Web crippling studies of SupaCee sections
456 under two flange load cases, Eng. Struct. 153 (2017) 582-597 2017.
457 [31] L. Sundararajah, M. Mahendran, P. Keerthan, Design of SupaCee sections subject to
458 web crippling under one-flange load cases, ASCE J of Structural Engineering 144 (12)
459 (2018), https://doi.org/10.1061/(ASCE)ST.1943-541X.0002206.
460 [32] L. Sundararajah, M. Mahendran, P. Keerthan, New design rules for lipped channel
461 beams subject to web crippling under two-flange load cases, Thin-Walled Structures.
462 119 (2017) 421-437 2017.
463 [33] L. Sundararajah, M. Mahendran, P. Keerthan, Numerical modelling and design of lipped
464 channel beams subject to web crippling under one-flange load cases, ASCE Journal of
465 Structural Engineering (07 January 2019), https://eprints.qut.edu.au/.
466 [34] L. Sundararajah, Web crippling studies of cold-Formed steel channel beams
467 experiments, numerical analyses and design rules, PhD Thesis Queensland University of
468 Technology, Brisbane, Australia, 2016.
469 [35] B. Young, G. Hancock, Design of cold-formed channel sections subjected to web
470 crippling, J. Struct. Eng. 127 (2001) 1137–1144.
471 [36] B. Janarthanan, L. Sundararajah, M. Mahendran, Web crippling behaviour and design of
472 cold-formed steel sections, Thin-Walled Structures, 2019, 140:387-403.

Notations	
b_f	Overall flange width of section
b_l	Overall lip width of section
R_P	Web crippling strength reduction factor
R_{p1}	Proposed web crippling strength reduction factor for the specimen under unfastened support condition
R_{p2}	Proposed web crippling strength reduction factor for the specimen under fastened support condition
R_{FEA}	Strength reduction factor predicted based on the results of finite element analysis
f_y	Yield strength
L	Length of the specimen
d	Overall web depth of section;
d_1	Depth of the flat portion of the web;
d_w	Width of the elongated web holes
b_w	Length of the elongated web holes
q	Length of edge-stiffener
Q	Ratio of the stiffener length to the depth of the flat portion of the web
D	Ratio of width of hole to depth of web
B	Aspect ratio of web hole
r_q	Inside fillet radius between web and hole edge-stiffener
r_i	Inside fillet radius of section
t	Thickness of the section
COV	Coefficient of variation
$P_{b,cr}$	Critical buckling load
$P_{b,y}$	Yield load
k	Critical buckling coefficient
v	Poisson's ratio
r_m	Inside fillet radius from mid-thickness line
N_m	Yield mechanism length
β	Reliability index
P_m	Load ratio's mean value
ϕ	Resistance factor

473

Appendix

Detials of specimens for elastic critical buckling analyses

d	r_i	t	N	d_w	b_w	r_q	q	$P_{b,cr}$	k_{FEA}	k_{prop}	k_{FEA}/k_{prop}
190	3.0	1.50	50	57	114.0	3.0	7.6	7.71	2.53	2.63	0.96
190	3.0	1.50	50	57	142.5	3.0	7.6	7.42	2.43	2.47	0.98
190	3.0	1.50	50	95	190.0	3.0	7.6	6.75	2.21	2.42	0.91
190	3.0	1.50	50	95	237.5	3.0	7.6	6.24	2.04	2.20	0.93
190	3.0	1.50	50	133	266.0	3.0	7.6	6.19	2.03	2.20	0.92
190	3.0	1.50	50	133	332.5	3.0	7.6	5.64	1.85	1.92	0.96
190	3.0	1.50	50	57	114.0	0	0	6.98	2.29	2.55	0.90
190	3.0	1.50	50	57	142.5	0	0	6.62	2.17	2.40	0.90
190	3.0	1.50	50	95	190.0	0	0	5.16	1.69	1.88	0.90
190	3.0	1.50	50	95	237.5	0	0	4.56	1.50	1.71	0.88
190	3.0	1.50	50	133	266.0	0	0	3.42	1.12	1.41	0.79
190	3.0	1.50	50	133	332.5	0	0	2.80	0.92	1.23	0.75
190	3.0	1.50	50	57	114.0	3.0	5.7	7.58	2.49	2.61	0.95
190	3.0	1.50	50	57	114.0	3.0	9.5	7.79	2.55	2.65	0.96
190	3.0	1.50	50	57	114.0	3.0	11.4	7.87	2.58	2.67	0.97
190	3.0	1.50	50	57	114.0	3.0	13.3	7.92	2.60	2.69	0.97
190	3.0	1.50	50	57	114.0	3.0	15.2	7.96	2.61	2.70	0.97
190	3.0	1.50	50	57	114.0	3.0	17.1	7.99	2.62	2.72	0.96
190	3.0	1.50	50	57	114.0	3.0	19.0	8.03	2.63	2.73	0.96
190	3.0	1.50	25	57	114.0	3.0	7.6	6.15	2.02	2.38	0.85
190	3.0	1.50	30	57	114.0	3.0	7.6	6.62	2.17	2.44	0.89
190	3.0	1.50	35	57	114.0	3.0	7.6	7.04	2.31	2.49	0.93
190	3.0	1.50	40	57	114.0	3.0	7.6	7.37	2.42	2.54	0.95
190	3.0	1.50	45	57	114.0	3.0	7.6	7.58	2.49	2.59	0.96
190	3.0	1.50	55	57	114.0	3.0	7.6	7.80	2.56	2.68	0.96
190	3.0	1.50	60	57	114.0	3.0	7.6	7.87	2.58	2.72	0.95
190	3.0	1.50	65	57	114.0	3.0	7.6	7.95	2.61	2.76	0.95
190	3.0	1.50	70	57	114.0	3.0	7.6	8.03	2.63	2.79	0.94
190	3.0	1.50	75	57	114.0	3.0	7.6	8.09	2.65	2.83	0.94
190	3.0	1.50	80	57	114.0	3.0	7.6	8.16	2.67	2.86	0.93
190	3.0	1.50	85	57	114.0	3.0	7.6	8.21	2.69	2.90	0.93
190	3.0	1.50	90	57	114.0	3.0	7.6	8.29	2.72	2.93	0.93
190	3.0	1.50	95	57	114.0	3.0	7.6	8.34	2.73	2.96	0.92
190	3.0	1.50	100	57	114.0	3.0	7.6	8.42	2.76	2.99	0.92
190	3.0	2.00	50	57	114.0	3.0	7.6	13.77	1.90	1.68	1.14
190	3.0	2.50	50	57	114.0	3.0	7.6	21.66	1.53	1.07	1.43
190	3.0	3.00	50	57	114.0	3.0	7.6	31.30	1.28	0.67	1.92
190	3.5	1.50	50	57	114.0	3.0	7.6	7.23	2.37	2.46	0.96
190	4.0	1.50	50	57	114.0	3.0	7.6	6.84	2.24	2.30	0.97
190	4.5	1.50	50	57	114.0	3.0	7.6	6.48	2.12	2.15	0.99
190	5.0	1.50	50	57	114.0	3.0	7.6	6.17	2.02	2.01	1.00
190	5.5	1.50	50	57	114.0	3.0	7.6	5.88	1.93	1.88	1.02
190	6.0	1.50	50	57	114.0	3.0	7.6	5.62	1.84	1.76	1.05
190	3.0	1.50	50	57	114.0	3.5	11.4	7.87	2.58	2.67	0.97
190	3.0	1.50	50	57	114.0	4.0	11.4	7.86	2.58	2.66	0.97
190	3.0	1.50	50	57	114.0	4.5	11.4	7.87	2.58	2.66	0.97
190	3.0	1.50	50	57	114.0	5.0	11.4	7.88	2.58	2.66	0.97
190	3.0	1.50	50	57	114.0	5.5	11.4	7.88	2.58	2.65	0.97
190	3.0	1.50	50	57	114.0	6.0	11.4	7.89	2.59	2.65	0.98

190	3.0	1.50	50	57	114.0	6.5	11.4	7.90	2.59	2.64	0.98
190	3.0	1.50	50	57	114.0	7.0	11.4	7.91	2.59	2.64	0.98
240	3.0	1.5	50	72	114.0	3.0	7.6	8.32	3.44	3.30	1.04
240	3.0	1.5	50	72	180.0	3.0	7.6	8.10	3.35	3.06	1.10
240	3.0	1.5	50	120	240.0	3.0	7.6	6.97	2.89	2.95	0.98
240	3.0	1.5	50	120	300.0	3.0	7.6	6.44	2.66	2.61	1.02
240	3.0	1.5	50	168	336.0	3.0	7.6	5.88	2.43	2.58	0.94
240	3.0	1.5	50	168	420.0	3.0	7.6	5.28	2.19	2.14	1.02
240	3.0	1.5	50	72	144.0	0	0	7.87	3.26	3.00	1.09
240	3.0	1.5	50	72	180.0	0	0	7.57	3.14	2.78	1.13
240	3.0	1.5	50	120	240.0	0	0	5.59	2.31	2.07	1.12
240	3.0	1.5	50	120	300.0	0	0	4.99	2.07	1.83	1.13
240	3.0	1.5	50	168	336.0	0	0	3.51	1.46	1.44	1.01
240	3.0	1.5	50	168	420.0	0	0	2.91	1.20	1.20	1.00
240	3.0	1.5	50	72	144.0	3.0	5.7	8.24	3.41	3.28	1.04
240	3.0	1.5	50	72	144.0	3.0	9.5	8.37	3.47	3.33	1.04
240	3.0	1.5	50	72	144.0	3.0	11.4	8.42	3.49	3.35	1.04
240	3.0	1.5	50	72	144.0	3.0	13.3	8.46	3.50	3.37	1.04
240	3.0	1.5	50	72	144.0	3.0	15.2	8.48	3.51	3.39	1.04
240	3.0	1.5	50	72	144.0	3.0	17.1	8.51	3.52	3.41	1.03
240	3.0	1.5	50	72	144.0	3.0	19	8.53	3.53	3.43	1.03
240	3.0	1.5	25	72	144.0	3.0	7.6	6.20	2.57	2.99	0.86
240	3.0	1.5	30	72	144.0	3.0	7.6	6.70	2.77	3.06	0.91
240	3.0	1.5	35	72	144.0	3.0	7.6	7.17	2.97	3.13	0.95
240	3.0	1.5	40	72	144.0	3.0	7.6	7.61	3.15	3.19	0.99
240	3.0	1.5	45	72	144.0	3.0	7.6	7.96	3.30	3.25	1.01
240	3.0	1.5	55	72	144.0	3.0	7.6	8.45	3.50	3.36	1.04
240	3.0	1.5	60	72	144.0	3.0	7.6	8.58	3.55	3.41	1.04
240	3.0	1.5	65	72	144.0	3.0	7.6	8.70	3.60	3.46	1.04
240	3.0	1.5	70	72	144.0	3.0	7.6	8.79	3.64	3.50	1.04
240	3.0	1.5	75	72	144.0	3.0	7.6	8.86	3.67	3.55	1.03
240	3.0	1.5	80	72	144.0	3.0	7.6	8.93	3.70	3.59	1.03
240	3.0	1.5	85	72	144.0	3.0	7.6	9.00	3.73	3.63	1.03
240	3.0	1.5	90	72	144.0	3.0	7.6	9.07	3.76	3.68	1.02
240	3.0	1.5	95	72	144.0	3.0	7.6	9.13	3.78	3.72	1.02
240	3.0	1.5	100	72	144.0	3.0	7.6	9.21	3.81	3.75	1.02
240	3.0	2.0	50	72	144.0	3.0	7.6	14.11	2.46	2.25	1.10
240	3.0	2.5	50	72	144.0	3.0	7.6	21.72	1.94	1.56	1.25
240	3.0	3.0	50	72	144.0	3.0	7.6	30.92	1.60	1.09	1.47
240	3.5	1.5	50	72	144.0	3.0	7.6	7.62	3.16	3.09	1.02
240	4.0	1.5	50	72	144.0	3.0	7.6	7.13	2.95	2.90	1.02
240	4.5	1.5	50	72	144.0	3.0	7.6	6.70	2.77	2.72	1.02
240	5.0	1.5	50	72	144.0	3.0	7.6	6.33	2.62	2.55	1.03
240	5.5	1.5	50	72	144.0	3.0	7.6	6.03	2.50	2.38	1.05
240	6.0	1.5	50	72	144.0	3.0	7.6	5.77	2.39	2.23	1.07
240	3.0	1.5	50	72	144.0	3.5	11.4	8.36	3.46	3.35	1.03
240	3.0	1.5	50	72	144.0	4.0	11.4	8.35	3.46	3.34	1.04
240	3.0	1.5	50	72	144.0	4.5	11.4	8.35	3.46	3.34	1.04
240	3.0	1.5	50	72	144.0	5.0	11.4	8.35	3.46	3.33	1.04
240	3.0	1.5	50	72	144.0	5.5	11.4	8.35	3.46	3.33	1.04
240	3.0	1.5	50	72	144.0	6.0	11.4	8.35	3.46	3.32	1.04
240	3.0	1.5	50	72	144.0	6.5	11.4	8.35	3.46	3.32	1.04
240	3.0	1.5	50	72	144.0	7.0	11.4	8.35	3.46	3.31	1.04

476